The NCA-1 ion channel functions downstream of G_q and Rho to regulate locomotion in *C. elegans*

Irini Topalidou[*], Pin-An Chen[†], Kirsten Cooper[*,1], Shigeki Watanabe[†,2], Erik M. Jorgensen[†], Michael Ailion[*]

[*]Department of Biochemistry, University of Washington, Seattle, WA 98195

[†]Howard Hughes Medical Institute, Department of Biology, University of Utah, Salt Lake City, UT 84112

[1]Current Address: Fred Hutchinson Cancer Research Center, Seattle, WA 98109

[2]Current Address: Department of Cell Biology, Johns Hopkins University, Baltimore, MD 21205

Running Title: Gq signaling activates NCA-1 through Rho

key words: G_q signaling, Rho small GTPase, NCA/NALCN ion channel, *C. elegans*, G protein

Corresponding author:

Michael Ailion

Department of Biochemistry

University of Washington

Box 357350

1705 NE Pacific St

Seattle, WA 98195

Phone: 206-685-0111

email: mailion@uw.edu

Abstract

The heterotrimeric G protein G_q positively regulates neuronal activity and synaptic transmission. Previously, the Rho guanine nucleotide exchange factor Trio was identified as a direct effector of G_q that acts in parallel to the canonical G_q effector phospholipase C. Here we examine how Trio and Rho act to stimulate neuronal activity downstream of G_q in the nematode *Caenorhabditis elegans*. Through two forward genetic screens, we identify the cation channel NCA-1/NALCN as a downstream target of the G_q/Rho pathway. By performing genetic epistasis analysis using dominant activating mutations and recessive loss-of-function mutations in the members of this pathway, we show that NCA-1 acts downstream of G_q in a linear pathway. Through cell-specific rescue experiments, we show that function of this channel in head acetylcholine neurons is sufficient for normal locomotion in *C. elegans*. Our results suggest that NCA-1 is a physiologically relevant target of neuronal G_q/Rho signaling in *C. elegans*.

Introduction

Heterotrimeric G protein pathways play central roles in altering neuronal activity and synaptic transmission in response to experience or changes in the environment. G_q is one of the four types of heterotrimeric G proteins alpha subunits in animals (Wilkie *et al.* 1992) and is widely expressed in the mammalian brain (Wilkie *et al.* 1991) where it typically acts to stimulate neuronal activity and synaptic transmission (Krause *et al.* 2002; Gamper *et al.* 2004; Coulon *et al.* 2010). These roles are conserved in the nematode *C. elegans*. Unlike mammals which have four members of the G_q family, *C. elegans* has only a single $G_q\alpha$ (Brundage *et al.* 1996). In *C. elegans*, loss-of-function and gain-of-function mutants in the single $G_q\alpha$ gene *egl-30* are viable but have strong neuronal phenotypes, affecting locomotion, egg-laying, and sensory behaviors (Brundage *et al.* 1996; Lackner *et al.* 1999; Bastiani *et al.* 2003; Matsuki *et al.* 2006; Esposito *et al.* 2010; Adachi *et al.* 2010). We aim to identify the signal transduction pathways and downstream targets by which G_q signaling alters neuronal activity.

In the canonical G_q pathway, G_q activates phospholipase Cβ (PLC) to cleave the lipid phosphatidylinositol 4,5,-bisphosphate (PIP2) into diacylglycerol (DAG) and inositol trisphosphate (IP3), each of which can act as a second messenger. This pathway operates in both worms and mammals, but in both systems, a number of PLC-independent effects of G_q have been described, indicating the existence of additional G_q signal transduction pathways (Lackner *et al.* 1999; Miller *et al.* 1999; Vogt *et al.* 2003; Bastiani *et al.* 2003; Sánchez-Fernández *et al.* 2014). Using a genetic screen for suppressors of activated G_q, we identified the Rho guanine nucleotide exchange factor (GEF) Trio as a direct effector of G_q in a second major G_q signal transduction pathway independent of the canonical PLC pathway (Williams *et al.* 2007). Biochemical and structural studies demonstrated that G_q directly binds and activates RhoGEF proteins in both worms and mammals, indicating that this new G_q pathway is conserved (Lutz *et al.* 2005; Williams *et al.* 2007; Lutz *et al.* 2007).

G_q activation of the Trio RhoGEF leads to activation of the small GTP-binding protein Rho, a major cellular switch that affects a number of cellular processes, ranging from regulation of the cytoskeleton to transcription (Etienne-Manneville and Hall 2002; Jaffe and Hall 2005). In *C. elegans* neurons, Rho has been shown to regulate synaptic transmission downstream of the G_{12}-class G protein GPA-12 via at least two pathways, one dependent on the diacylglycerol kinase DGK-1 and one independent of DGK-1 (McMullan *et al.* 2006; Hiley *et al.* 2006). Here we investigate what targets operate downstream of Rho in the G_q signaling pathway to regulate neuronal activity. Through two forward genetic screens, we identify the cation channel NCA-1 (NALCN in mammals) as a downstream target of the G_q/Rho pathway. The NCA-1/NALCN channel is a relative of voltage-gated cation channels that has been suggested to be a sodium leak channel required for the propagation of neuronal excitation and the fidelity of synaptic transmission (Lu *et al.* 2007; Jospin *et al.* 2007; Yeh *et al.* 2008). However, there is controversy over the current carried by NALCN and whether it is indeed a sodium leak channel (Senatore *et al.* 2013; Senatore and Spafford 2013; Boone *et al.* 2014). It is also unclear how NALCN is gated and what pathways activate the channel. Two studies have shown that NALCN-dependent currents can be activated by G protein-coupled receptors, albeit independently of G proteins (Lu *et al.* 2009; Swayne *et al.* 2009), and another study showed that the NALCN leak current can be activated by low extracellular calcium via a G protein-dependent pathway (Lu *et al.* 2010). Our data presented here suggest that NCA-1 can be activated by Rho acting downstream of G_q in a linear pathway.

Materials and Methods

Strains

Worm strains were cultured and maintained using standard methods (Brenner, 1974). A complete list of strains and mutations used is provided in the strain list (Table S1).

Isolation of suppressors of activated G_q

We performed an ENU mutagenesis to screen for suppressors of the hyperactive locomotion of an activated G_q mutant, *egl-30(tg26)* (Ailion *et al.* 2014). From approximately 47,000 mutagenized haploid genomes, we isolated 10 mutants that had a fainter phenotype when outcrossed away from the *egl-30(tg26)* mutation. By mapping and complementation testing, we assigned these ten mutants to three genes: three *unc-79* mutants (*yak37*, *yak61*, and *yak73*), six *unc-80* mutants (*ox329*, *ox330*, *yak8*, *yak35*, *yak36*, and *yak56*) and one *nlf-1* mutant (*ox327*).

Isolation of suppressors of activated G_o

We first isolated suppressors of the activated G_o mutant *unc-109(n499)* by building double mutants of *unc-109(n499)* with the activated G_q allele *egl-30(tg26)*. Unlike *unc-109(n499)* homozygotes which are lethal, *egl-30(tg26) unc-109(n499)* homozygotes are viable, but paralyzed and sterile, indicating that activated G_q partially suppresses activated G_o, consistent with the model that these two G proteins act antagonistically. We built a balanced heterozygote strain *egl-30(tg26) unc-109(n499)/egl-30(tg26) unc-13(e51) gld-1(q126)* which has an “unmotivated” phenotype in which the worms move infrequently and slowly. We mutagenized these animals with ENU and screened for F1 progeny that moved better. From a screen of approximately 16,000 mutagenized haploid genomes, we isolated two apparent *unc-109* intragenic mutants, *ox303* and *ox304*. *ox303* is a strong *unc-109* loss-of-function allele, as evidenced by the fact that *egl-30(tg26) unc-109(n499 ox303)/egl-30(tg26) unc-13(e51) gld-1(q126)* mutants resembled *egl-30(tg26)*

mutants (i.e. hyperactive). Additionally, *unc-109(n499 ox303)* mutants themselves are hyperactive in an otherwise wild-type background. *ox304*, however, appears to be a partial loss-of-function mutant, because the *egl-30(tg26) unc-109(n499 ox304)/egl-30(tg26) unc-13(e51) gld-1(q126)* mutant moves better than the *egl-30(tg26) unc-109(n499)/egl-30(tg26) unc-13(e51) gld-1(q126)* parent strain, but is not hyperactive like the *egl-30(tg26)* strain. Also, *unc-109(n499 ox304)* homozygote animals on their own are viable but are almost paralyzed and show very little spontaneous movement, with a typical straight posture. However, when stimulated by transfer to a new plate, the *unc-109(n499 ox304)* mutant is surprisingly capable of coordinated movements. This strain was used for mapping and sequencing experiments that demonstrated that *unc-109* is allelic to *goa-1*, encoding the worm G_o ortholog (see below). The *unc-109(n499 ox304)* strain was also used as the starting point for a second screen to isolate extragenic suppressors of activated G_o.

Previously, a screen for suppressors of activated *goa-1* was performed using heat-shock induced expression of an activated *goa-1* transgene (Hajdu-Cronin *et al.* 1999). This screen isolated many alleles of *dgk-1*, encoding diacyclglycerol kinase, but only a single allele of *eat-16*, encoding a regulator of G protein signaling (RGS) protein that negatively regulates G_q (Hajdu-Cronin *et al.* 1999), along with mutants in three genes needed for expression of the heat-shock *goa-1* transgene (Hajdu-Cronin *et al.* 2004). Because of the strong bias of this screen for isolating alleles of *dgk-1*, we used the *goa-1(n499 ox304*) strain to perform a screen for suppressors of activated G_o that did not involve overexpression of *goa-1* or rely on expression of a heat-shocked induced *goa-1* transgene. We performed ENU mutagenesis of *goa-1(n499 ox304*) and isolated F2 animals that were not paralyzed. From a screen of approximately 24,000 mutagenized haploid genomes, we isolated 17 suppressors, 9 with a relatively stronger suppression phenotype and 8 that were weaker. Of the 9 stronger suppressors, we isolated two alleles of *eat-16* (*ox359*, *ox360*), three alleles of the BK type potassium channel *slo-1* (*ox357*, *ox358*, *ox368*), one allele of the innexin *unc-9* (*ox353*), one gain-of-function allele in the ion channel gene *nca-1* (*ox352*), and two

mutants that were mapped to chromosomal regions distinct from the other mutations listed above, but not further characterized (*ox356*, *ox364*).

Mapping and cloning *unc-109(n499)*

unc-109 was shown to be allelic to *goa-1*. First, we performed SNP mapping of both *unc-109(n499)* and its intragenic revertant *unc-109(n499 ox303)*, using the Hawaiian strain CB4856 as described (Davis *et al.* 2005). These experiments mapped *unc-109* to an approximately 1 Mb region in the middle of chromosome I between SNPs on cosmids D2092 and T24B1 (SNPs CE1-15 and T24B1[1]). A good candidate in this region was *goa-1*. We confirmed that *unc-109* was indeed *goa-1* by sequencing the three *unc-109* mutants: the gain-of-function allele *n499* carries a point mutation that leads to an R179C missense mutation, affecting a conserved arginine residue shown to be important for the GTPase activity of G proteins (Coleman *et al.* 1994); the partial loss-of-function allele *ox304* carries a point mutation leading to a W259R missense mutation; and the strong loss-of-function allele *ox303* carries a one basepair deletion that leads to a premature stop 32 amino acids from the C-terminal.

Mapping and cloning *nlf-1(ox327)*

We mapped the *ox327* mutation using single nucleotide polymorphisms (SNPs) in the Hawaiian strain CB4856 as described (Davis et al., 2005). The *ox327* mutation was mapped to an approximately 459 kb region on the left arm of the X chromosome between SNPs on cosmids F39H12 and C52B11 (SNPs F39H12[4] and pkP6101). This region included 74 predicted protein-coding genes. We injected cosmids spanning this region and found that injection of cosmid F55A4 rescued the *ox327* mutant phenotype. We performed RNAi to the genes on this cosmid in the *eri-1(mg366) lin-15(n744)* strain that has enhanced RNAi and found that RNAi of the gene F55A4.2 caused a weak fainter phenotype. We sequenced F55A4.2 in the *ox327* mutant and found a T to A transversion mutation in exon 1, leading to a premature stop codon at amino acid C59. We also

rescued the *ox327* mutant with a transgene carrying only F55A4.2, confirming the gene identification. We subsequently obtained a deletion allele *tm3631* that has fainter and G_q suppression phenotypes indistinguishable from *ox327*. F55A4.2 was given the gene name *nlf-1* (Xie *et al.* 2013).

We obtained six independent *nlf-1* cDNAs that were predicted to be full-length: yk1105g4, yk1159a2, yk1188d11, yk1279a1, yk1521f8, and yk1709b10. Restriction digests suggested that all six were of the same size. We sequenced yk1159a2 and yk1279a1 and both gave the same *nlf-1* exon-intron structure, which differed from the gene-structure on Wormbase WS253 in several ways: *nlf-1* is 4 bp shorter at the 3' end of exon 5, and has a new 154 bp exon (now exon 6) not predicted on Wormbase. *nlf-1* consists of 8 exons and is predicted to encode a protein of 438 amino acids. This is identical to the gene structure reported independently (Xie *et al.* 2013). Both sequenced cDNAs had 5'UTRs of 64 bp, with yk1159a2 (but not yk1279a1) being trans-spliced to the SL1 splice leader, and 3'UTRs of 424 bp (yk1279a1) or 429 bp (yk1159a2). The yk1279a1 cDNA was mutation-free and was cloned into a Gateway entry vector for use in rescue experiments. The full-length sequence of the yk1279a1 *nlf-1* cDNA was deposited in GenBank under accession # KX808524.

Molecular biology and transgenes

A complete list of constructs is provided in the plasmid list (Table S2). Most of the constructs were made using the three slot multisite Gateway system (Invitrogen). For C3 transferase constructs, a promoter, an FRT-mCherry-FRT-GFP cassette (pWD178), and the C3 transferase-*unc-54* 3'UTR (cloned into a Gateway entry vector from plasmid QT#99) were combined into the pDEST R4-R3 destination vector. For *nlf-1* tissue-specific rescue constructs, a promoter, the *nlf-1* coding sequence (genomic DNA or cDNA), and a C-terminal GFP tag were cloned along with the *unc-54* 3'UTR into the pDEST R4-R3 destination vector. Promoters used were *nlf-1p* (5.7 kb upstream of the ATG), *rab-3p* (all neurons), *unc-17p* (acetylcholine neurons),

193 *unc-17Hp* (head acetylcholine neurons) (Hammarlund *et al.* 2007), *acr-2p* (acetylcholine motor
194 neurons), *unc-17βp* (acetylcholine motor neurons) (Charlie *et al.* 2006), and *glr-1p* (glutamate-
195 receptor interneurons). Extrachromosomal arrays were made by standard transformation methods
196 (Mello *et al.* 1991). Constructs of interest were injected at 10 ng/μl with marker and carrier DNAs
197 added to make a final total concentration of at least 100 ng/μl. For most constructs, we isolated
198 multiple independent insertions that behaved similarly. C3 transferase extrachromosomal arrays
199 were integrated into the genome using X-ray irradiation (4000 rads). Integrated transgenes were
200 mapped to chromosomes and outcrossed twice before further analysis.
201
202 **Locomotion assays**
203 We performed two different assays to measure locomotion. Body bend assays measured
204 the rate of locomotion. Radial locomotion assays measured the radial distance animals moved
205 from a point in a given unit of time, which provides a combined measurement of different aspects
206 of the locomotion phenotype including the rate of locomotion, waveform, and frequency of
207 reversals. Both types of assays were performed on 10 cm plates seeded with thin lawns of OP50
208 bacteria. These plates were prepared by seeding 1.5 ml of stationary phase OP50 bacteria to
209 evenly cover the entire plate surface, and then growing the bacteria for two days at room
210 temperature. Plates were stored at 4° for up to one month before being used. For body bend
211 assays, first-day adult worms were picked to an assay plate, allowed to rest for 30 seconds, and
212 then body bends were counted for one minute. A body bend was defined as the movement of the
213 worm from maximum to minimum amplitude of the sine wave (Miller *et al.* 1999). To minimize
214 variation, all animals in a body bend experiment were assayed on the same plate. For radial
215 locomotion assays, five to eight first-day adults were picked together to the center of a plate to
216 begin the assay (time 0). Positions of the worms were marked on the lid of the plate every ten
217 minutes for up to forty minutes. Following the assay, the distance of each point to the center was

measured. For most strains, radial distances did not increase after the first ten minutes of the assay and all data presented here are for the ten-minute time point. Analysis of the data at later time points leads to the same conclusions. For all locomotion assays, the experimenter was blind to the genotypes of the strains being assayed.

For Rho inhibition experiments (Figure 1), expression of C3 transferase (C3T) was induced by FLP-mediated recombination. Expression of FLP was induced by heat shock for 1 hr at 34°C, plates were returned to room temperature, and animals were scored for locomotion 4 hrs after the end of the heat shock period. For heat-shock induction of activated Rho (Figure S5), worms were heat shocked for 1 hr at 34°C, returned to room temperature, and scored for locomotion 2 hrs after the end of the heat-shock period.

Fainting assays

Backward fainting times were measured by touching a worm on the head with a worm pick to stimulate movement, and measuring the time to faint with a stopwatch. Forward fainting time was measured following a touch on the tail. Fainting was defined by an abrupt stop of movement along with a characteristic straightening of the head (see Figure 5). Alternatively, we touched worms on the head or tail with a pick and counted the number of body bends until the worm fainted. If a worm moved 10 body bends without fainting, we stopped the assay.

Imaging and image analysis

Worms were mounted on 2% agarose pads and anesthetized with sodium azide. Images were obtained using a Zeiss Pascal confocal microscope. For quantitative imaging of NCA-1::GFP and NCA-2::GFP (Figure S2), Z-stack projections of the nerve ring axons on one side of the animal were collected and quantified in ImageJ as described (Jospin *et al.* 2007). Dissecting microscope photographs of first-day adult worms were taken at 50X using a Nikon SMZ18 microscope equipped with a DS-L3 camera control system.

Statistics

P values were determined using GraphPad Prism 5.0d (GraphPad Software). Normally distributed data sets with multiple comparisons were analyzed by a one-way ANOVA followed by a Bonferroni or Tukey posthoc test to examine selected comparisons or by Dunnett's test if all comparisons were to the wild type control. Non-normally distributed data sets with multiple comparisons were analyzed by a Kruskal-Wallis nonparametric ANOVA followed by Dunn's test to examine selected comparisons. Pairwise data comparisons were analyzed by a two-tailed unpaired t test for normally distributed data or by a two-tailed Mann-Whitney test for non-normally distributed data.

Reagent and data availability

Strains and plasmids are shown in Table S1 and Table S2 and are available from the *Caenorhabditis* Genetics Center (CGC) or upon request. The full-length sequence of the yk1279a1 *nlf-1* cDNA was deposited in GenBank under accession # KX808524. The authors state that all data necessary for confirming the conclusions presented in the article are represented fully within the article and Supplemental Material.

Results

Inhibition of Rho suppresses activated G_q

Two pieces of data suggested that G_q may regulate locomotion in *C. elegans* through activation of the small G protein Rho. First, both the hyperactive locomotion and tightly wound body posture of the activated G_q mutant *egl-30(tg26)* are suppressed by loss-of-function mutations in the *unc-73* RhoGEF Trio, an activator of Rho (Williams *et al.* 2007). Second, expression of activated Rho as a transgene causes worms to adopt a posture characterized by a tightly coiled, high-amplitude waveform (McMullan *et al.* 2006), reminiscent of the waveform of activated G_q worms (Bastiani *et al.* 2003; Ailion *et al.* 2014). To determine directly whether G_q signals through Rho, we tested whether Rho inhibition suppresses an activated G_q mutant.

In *C. elegans,* there is a single gene encoding Rho (*rho-1*). Loss of *rho-1* causes numerous pleiotropic developmental phenotypes and embryonic lethality (Jantsch-Plunger *et al.* 2000). Thus, to bypass the developmental roles and study Rho function in the adult nervous system, we expressed the Rho inhibitor C3 transferase (C3T) only in adult neurons by using the FLP recombinase/FRT system (Davis *et al.* 2008). In this system, temporal control of C3T is achieved through induction of FLP via heat-shock. FLP in turn promotes recombination between FRT sites to lead to expression of C3 transferase in specific neurons (Figure 1A). We expressed C3T in the following classes of neurons: all neurons (*rab-3p*), acetylcholine neurons *(unc-17p*), head acetylcholine neurons (*unc-17Hp*), and acetylcholine motor neurons (*unc-17βp*). mCherry fluorescence confirmed expression in the expected neurons and GFP expression was used to monitor induction of C3T following FLP-mediated recombination.

Inhibition of *rho-1* in adult neurons caused a decreased locomotion rate (Figure 1B). This effect was greatest when Rho was inhibited in all neurons, but Rho inhibition in acetylcholine subclasses of neurons also led to slower locomotion. Thus, Rho acts in multiple classes of neurons to promote locomotion in adult worms. In the absence of heat-shock, all strains showed

normal wild-type rates of locomotion and did not express any detectable GFP, indicating that these transgenes do not provide leaky expression of C3T in the absence of heat-shock. This confirms that Rho acts post-developmentally in mature neurons to regulate locomotion behavior (McMullan *et al.* 2006).

To determine whether Rho acts downstream of G_q signaling, we crossed the C3 transgenes into the background of the activated G_q mutant *egl-30(tg26)*. Inhibition of *rho-1* in all adult neurons suppressed both the posture and hyperactive locomotion of the activated G_q mutant (Figure 1C,D). Inhibition of *rho-1* in acetylcholine neurons suppressed the hyperactivity of activated G_q (Figure 1C), but the worms still had a coiled, high-amplitude waveform (Figure 1D). Thus, *rho-1* exhibits genetic interactions consistent with a role in the G_q signaling pathway.

Mutations in NCA channel subunits suppress activated G_q

What acts downstream of Rho in the G_q signal transduction pathway? We screened for suppressors of activated Gq and found mutants in three categories: (1) the canonical G_q pathway (such as the PLC *egl-8*); (2) the RhoGEF *unc-73* (Williams *et al.* 2007), and (3) genes that affect dense-core vesicle function (*e.g. unc-31*, *rab-2*, *rund-1*) (Ailion *et al.* 2014; Topalidou *et al.* 2016). Mutations in *unc-73* strongly suppress the high-amplitude waveform of the activated G_q mutant, but mutations in the canonical G_q pathway or in genes that affect dense-core vesicle function only weakly suppress the high-amplitude waveform of the activated G_q mutant (Figure S1). Thus, strong suppression of the high-amplitude waveform of activated G_q may be a specific characteristic of mutations in the Rho pathway, and we hypothesized that downstream targets of Rho in this pathway would also suppress the high-amplitude waveform.

To identify possible downstream targets of Rho in the G_q pathway, we examined other mutants isolated from our screen for suppression of the high-amplitude waveform of activated G_q (Figure S1). When crossed away from the activating G_q mutation, several of these mutants had a "fainter" phenotype. Fainter mutants respond to a touch stimulus by moving away, but abruptly

stop, that is “faint”, after only a few body bends. The fainter phenotype has been observed only in mutants that reduce the function of the NCA-1 and NCA-2 ion channels (Humphrey *et al.* 2007; Jospin *et al.* 2007; Yeh *et al.* 2008). We found that all our G_q suppressors that strongly suppressed the high-amplitude waveform and had a fainter phenotype were mutants in either *unc-79* or *unc-80*, two genes required for function of the NCA channels (Humphrey *et al.* 2007; Jospin *et al.* 2007; Yeh *et al.* 2008). We also isolated a single mutant in the gene *nlf-1* that only weakly suppressed the high-amplitude waveform of activated G_q (Figure S1), but also gave fainters after outcrossing away from the activated G_q mutation. *unc-79* and *unc-80* mutants have a strong fainter phenotype, equivalent to that of a double mutant in *nca-1* and *nca-2*, two genes that encode pore-forming subunits of the NCA channels in *C. elegans* (Humphrey *et al.* 2007; Jospin *et al.* 2007; Yeh *et al.* 2008). Like *unc-79* or *unc-80*, an *nca-1 nca-2* double mutant suppressed the activated G_q mutant. Additionally, *nca-1* on its own suppressed activated G_q, but *nca-2* did not. This suggests that although *nca-1* and *nca-2* are only redundantly required for normal worm locomotion, G_q activation may be specific to channels containing the NCA-1 pore-forming subunit.

Cloning and characterization of *nlf-1(ox327)*

In addition to the previously known NCA channel subunits *unc-79* and *unc-80*, we also isolated the *ox327* mutant in a gene that had not been previously characterized at the time of our study. We cloned *ox327* by single nucleotide polymorphism (SNP) mapping, RNAi and transgenic rescue experiments (see Materials and Methods), showing that it carries an early stop mutation in the gene *nlf-1*. The *nlf-1(ox327)* and *nlf-1(tm3631)* deletion mutants failed to complement each other and had indistinguishable fainting and G_q suppression phenotypes. *nlf-1* was independently identified by others and encodes an endoplasmic reticulum-localized protein probably involved in proper assembly of the NCA channel, since *nlf-1* mutants had reduced expression levels of GFP-tagged NCA-1 and NCA-2 (Xie *et al.* 2013). We also found that *nlf-1* is required for normal axonal levels of both GFP-tagged NCA-1 and NCA-2 in the nerve ring (Figure S2). Additionally, an *nlf-1*

mutation strongly suppressed both the slow locomotion and coiled posture of an activated *nca-1* mutant (Figure 2), demonstrating that *nlf-1* is important for NCA-1 function.

nlf-1 mutants have a weaker fainter phenotype than mutants of *unc-79* or *unc-80*, or the *nca-1 nca-2* double mutant. The *nlf-1* fainting phenotype differs in two ways from those of the stronger fainting mutants. First, *nlf-1* mutants take a longer time to faint following stimulation (Figure 3). Second, while the strong fainting mutants show a similarly strong fainting phenotype in either the forward or backward direction, *nlf-1* mutants faint reliably in the backward direction but take much longer and have more variable fainting in the forward direction (Figure 3), suggesting that *nlf-1* mutations cause a partial loss of function of the NCA channels. Additionally, *nlf-1* mutants have greater spontaneous locomotion activity than *unc-79*, *unc-80* or *nca-1 nca-2* double mutants. To determine how *nlf-1* interacts with NCA mutants, we built *nlf-1(ox327)* double mutants with *unc-79, unc-80*, *nca-1* and *nca-2*. The *nlf-1* mutation did not enhance the *unc-79* or *unc-80* fainter phenotype, suggesting that these mutants act in the same pathway to control fainting. However, *nca-1* strongly enhanced the *nlf-1* fainter phenotype, while *nca-2* had a weak effect on *nlf-1* fainting that was not statistically significant (Figure 3). Neither *nca-1* nor *nca-2* single mutants have a fainter phenotype on their own, but the fact that an *nca-1 nlf-1* double mutant has a strong fainter phenotype suggests that either *nca-1* contributes more than *nca-2* for normal locomotion or that *nlf-1* specifically perturbs function of *nca-2*. Our data presented below are more consistent with the possibility that *nca-1* contributes more than *nca-2* to wildtype locomotion behavior.

We determined the cellular expression pattern of *nlf-1* by fusing its promoter to GFP. *nlf-1p::GFP* was expressed in most or all neurons, but was not detected in other tissues (Figure S3). This agrees with the expression pattern reported elsewhere (Xie *et al.* 2013). To determine the neuronal focus of the fainter phenotype, we performed rescue experiments in which we determined whether an *nlf-1* mutant could be rescued by expression of a wild-type *nlf-1* cDNA under the control of neuron-specific promoters. Expression of *nlf-1(+)* in all neurons (using the *rab-3* promoter) or acetylcholine neurons (using the *unc-17* promoter) fully rescued the *nlf-1* mutant

fainter phenotype (Figure 4A). Expression in acetylcholine motor neurons (using the *acr-2* or *unc-17β* promoters) did not rescue the fainter phenotype, but expression driven by a head-specific derivative of the *unc-17* promoter (*unc-17Hp*) fully rescued the fainter phenotype, indicating that the action of *nlf-1* in head acetylcholine neurons is sufficient to prevent fainting (Figure 4A).

Previously, it was reported that expression of *nlf-1* in premotor interneurons is sufficient to rescue the *nlf-1* mutant fainter phenotype (Xie *et al.* 2013). However, we found that expression of *nlf-1* in premotor interneurons using the *glr-1* promoter (*glr-1p*) only partially rescued the *nlf-1* mutant fainter phenotype and did not fully restore wild-type locomotion (Figure 4B). Fainting behavior was difficult to score in the *glr-1* promoter-rescued *nlf-1* mutant animals because they had sluggish movement and stopped frequently, though generally not with the suddenness and characteristic posture typical of fainters. Though we could blindly score the rescue of fainting in these animals by eye, we saw only weak rescue of the *nlf-1* mutant by *glr-1* promoter expression in our quantitative fainting assays and the effect was not statistically significant (Figure 4B). When we instead measured fainting as the percentage of animals that fainted within ten body bends, we did see a marginally significant rescue by *glr-1* promoter expression (backward fainting: *nlf-1* = 92%, *nlf-1; glr-1p::nlf-1(+)* = 68%, P=0.0738, Fisher's exact test; forward fainting: *nlf-1* = 80%, *nlf-1; glr-1p::nlf-1(+)* = 48%, P=0.0378, Fisher's exact test). We may be underestimating the rescue of the fainting phenotype by *glr-1* promoter expression due to the difficulty distinguishing the frequent pausing from true fainting. Nevertheless, rescue of the *nlf-1* mutant is clearly stronger by expression in head acetylcholine neurons using the *unc-17H* promoter (Figure 4A). Though our data seem to contradict the previous study reporting that *nlf-1* acts in premotor interneurons (Xie *et al.* 2013), there are several possible explanations. First, like our data, the data in the previous study in fact showed only partial rescue of fainting behavior by expression in premotor interneurons (Xie *et al.* 2013). Second, the premotor interneuron promoter combination used in the previous study (*nmr-1p* + *sra-11p*) leads to expression in several other head interneurons that may contribute to the phenotype. Third, it is possible that rescue is sensitive to expression level

and that different levels of expression were achieved in the two studies, leading to different levels of rescue. We conclude that NLF-1 acts in head acetylcholine neurons, including the premotor interneurons, to promote sustained locomotion in the worm. Consistent with this, the premotor command interneurons have recently been shown to have acetylcholine (Pereira *et al.* 2015).

Mutations in NCA channel subunits suppress activated Rho

To determine whether NCA mutants act downstream of Rho, we took advantage of an activated Rho mutant (G14V) expressed specifically in the acetylcholine neurons (McMullan *et al.* 2006). Like an activated G_q mutant, this activated Rho mutant has an exaggerated waveform. We built double mutants of the activated Rho mutant with mutations in *unc-79*, *unc-80*, *nlf-1* and mutations in the NCA channel subunit genes *nca-1* and *nca-2*. The *nca-1* and *nca-2* genes are redundant for the fainter phenotype because neither mutant has a fainter phenotype individually, but the double mutant has a fainter phenotype indistinguishable from *unc-79* and *unc-80* mutants (Humphrey *et al.* 2007; Jospin *et al.* 2007; Yeh *et al.* 2008). We found that mutations in *unc-79* or *unc-80* strongly suppressed the high-amplitude waveform of activated Rho, as did an *nca-1 nca-2* double mutant (Figure 5). In all cases, the resulting double (or triple) mutants had a fainter phenotype like the single mutants. By contrast, a mutation in *nlf-1* strongly but incompletely suppressed the high-amplitude waveform of activated Rho, consistent with the *nlf-1* mutation causing a partial but incomplete loss of NCA channel function. Unlike an *nlf-1* single mutant, an *nlf-1* double mutant with activated Rho did not have a fainter phenotype. Additionally, a mutation in *nca-1* also strongly but incompletely suppressed the high-amplitude waveform of activated Rho, but a mutation in *nca-2* did not suppress the high-amplitude waveform (Figure 5). Thus, activated Rho may signal primarily through NCA channels formed from the NCA-1 pore-forming subunit.

Because an activated Rho mutant has slow locomotion (Figure 6) and *unc-79*, *unc-80*, and *nca-1 nca-2* double mutants also have slow locomotion, it is difficult to determine whether these NCA channel mutants suppress the locomotion phenotype of activated Rho in addition to its

417 waveform. We performed radial locomotion assays that provide a combined measurement of
418 several aspects of the locomotion phenotype, including the rate of movement, frequency of
419 reversals, and amplitude of the waveform (see Materials and Methods). By these assays,
420 mutations in *unc-80* or *nca-1 nca-2* lead to only small increases in the radial distance traveled by
421 an activated Rho mutant and an *nca-2* mutant had no effect (Figure S4). However, a mutation in
422 *nlf-1* much more strongly increased the radial distance traveled by an activated Rho mutant.
423 Because the *nlf-1* mutant is not as slow on its own, we could also directly assay its effect on the
424 rate of locomotion of an activated Rho mutant by counting the number of body bends per minute.
425 An *nlf-1* mutation strongly increased the rate of locomotion of an activated Rho mutant (Figure 6).
426 In fact, the *nlf-1* double mutant with activated Rho had a faster rate of locomotion than either
427 activated Rho or *nlf-1* on its own, similar to the effect of *nlf-1* on the locomotion of an activated
428 *nca-1* mutant (Figure 2B). Additionally, a mutation in *nca-1* strongly increased the locomotion rate
429 of the activated Rho mutant, but a mutation in *nca-2* had no effect (Figure 6), further supporting
430 the idea that NCA channels consisting of the NCA-1 subunit act downstream of G_q and Rho in this
431 pathway.

432 Rho regulates worm locomotion independently of effects on development, as demonstrated
433 by the fact that heat-shock induction of an activated Rho transgene in adults leads to a high-
434 amplitude waveform similar to that seen in worms that express activated Rho in acetylcholine
435 neurons (McMullan *et al.* 2006). Consistent with the idea that NCA-1 acts downstream of Rho,
436 mutations in the fainter genes *unc-79*, *unc-80*, and *nlf-1* suppress the high-amplitude waveform
437 phenotype of heat-shock induced activated Rho (Figure S5A). Additionally, *nlf-1* also suppresses
438 the locomotion defect of heat-shock induced activated Rho (Figure S5B). Thus, Rho regulates
439 worm locomotion via NCA-1 by acting in a non-developmental pathway that operates in adult
440 neurons.

441

442 **A dominant NCA-1 mutation suppresses activated G_o**

In *C. elegans*, the G_q pathway is opposed by signaling through the inhibitory G_o protein GOA-1 (Hajdu-Cronin *et al.* 1999; Miller *et al.* 1999). Thus, loss-of-function mutants in *goa-1* are hyperactive and have a high-amplitude waveform, similar to the gain-of-function G_q mutant *egl-30(tg26)*. We found that the uncloned dominant mutant *unc-109(n499)* which is paralyzed and resembles loss-of-function mutants in *egl-30* (Park and Horvitz 1986) carries an activating mutation in *goa-1* (see Materials and Methods). The *goa-1(n499)* mutant is paralyzed as a heterozygote, and is lethal as a homozygote (Park and Horvitz 1986). We performed a screen for suppressors of *goa-1(n499)* and isolated a partial intragenic suppressor, *goa-1(n499 ox304*) (Materials and Methods). The *goa-1(n499 ox304)* mutant has a strong movement defect similar to *goa-1(n499)*, but is viable as a homozygote and thus easier to work with than *goa-1(n499)*.

We used the *goa-1(n499 ox304*) strain to perform a screen for suppressors of activated G_o (Materials and Methods). Among the suppressors, we isolated a mutant (*ox352*) that was found to be a dominant gain-of-function mutation in the *nca-1* gene (Fig. 2A, Chen et al., personal communication). Thus, activation of NCA-1 suppresses activated G_o whereas loss of NCA-1 suppresses activated G_q, both consistent with the model that G_o inhibits G_q and that NCA-1 is a downstream effector of the G_q pathway.

Discussion

In this study, we identify the NCA-1 ion channel as a downstream effector of the heterotrimeric G protein G_q. Our genetic epistasis data indicate that G_q activates the RhoGEF Trio and the small GTPase Rho. Rho then acts via an unknown mechanism to activate the NCA-1 ion channel, which is required for normal neuronal activity and synaptic transmission in *C. elegans* (Jospin *et al.* 2007; Yeh *et al.* 2008; Xie *et al.* 2013; Gao *et al.* 2015). Thus, this work identifies a new genetic pathway from G_q to an ion channel that regulates neuronal excitability and synaptic release: G_q → RhoGEF → Rho → NCA-1 (Figure 7). NCA-1 has not been previously identified as an effector of the G_q pathway, so this pathway may give insight into how NCA-1 is activated or regulated.

Mutants that eliminate the NCA channels such as *unc-80* or the *nca-1 nca-2* double mutant completely suppress the locomotion and body posture phenotypes of an activated Rho mutant (Figure 5, Figure S4), suggesting that NCA channels act downstream of Rho in a linear pathway. Additionally, channels composed of the pore-forming subunit NCA-1 may be the main target of G_q/Rho signaling. First, loss-of-function mutations in *nca-1* but not *nca-2* partially suppress activated G_q and activated Rho mutants. Second, activating gain-of-function mutants of *nca-1* have phenotypes reminiscent of activated G_q and activated Rho mutants, but no activated mutants in *nca-2* have been isolated. Third, loss-of-function mutations in *nca-1* but not *nca-2* enhance the weaker fainting phenotype of an *nlf-1* mutant which does not fully eliminate function of the NCA channels. Together, these data suggest that although either NCA-1 or NCA-2 activity is sufficient for wild-type locomotion, NCA-1 is likely to be the target of G protein regulation.

It is not clear, however, whether Rho activation of NCA-1 is direct or indirect. G_q directly interacts with and activates the RhoGEF and Rho, as shown by the crystal structure of a complex between $G_q\alpha$, RhoGEF, and Rho (Lutz *et al.* 2007). Rho is known to have many possible effectors and actions in cells (Etienne-Manneville and Hall 2002; Jaffe and Hall 2005). In *C. elegans* neurons, Rho has been previously shown to regulate synaptic transmission via at least two

pathways, one involving a direct interaction of Rho with the DAG kinase DGK-1 and one that is DGK-1 independent (McMullan *et al.* 2006). A candidate for the link between Rho and NCA-1 is the type I phosphatidylinositol 4-phosphate 5-kinase (PIP5K) that synthesizes the lipid phosphatidylinositol 4,5,-bisphosphate (PIP2). PIP5K is an intriguing candidate for several reasons. First, activation of G_q in mammalian cells has been shown to stimulate the membrane localization and activity of PIP5K via a mechanism that depends on Rho (Chatah and Abrams 2001; Weernink *et al.* 2004). Second, in *C. elegans*, mutations eliminating either the NCA channels (*nca-1 nca-2* double mutant) or their accessory subunits (*unc-79* or *unc-80*) suppress mutants in the PIP2 phosphatase synaptojanin (*unc-26*) and also suppress phenotypes caused by overexpression of the PIP5K gene *ppk-1* (Jospin *et al.* 2007). Loss of a PIP2 phosphatase or overexpression of a PIP5K are both predicted to increase levels of PIP2. Since loss of NCA channels suppresses the effects of too much PIP2, it is possible that excessive PIP2 leads to overactivation of NCA channels and that PIP2 might be part of the normal activation mechanism. There are numerous examples of ion channels that are regulated or gated by phosphoinositide lipids such as PIP2 (Balla 2013).

The NCA/NALCN ion channel was discovered originally by bioinformatic sequence analyses (Lee *et al.* 1999; Littleton and Ganetzky 2000). It is conserved among all metazoan animals and is evolutionarily-related to the family of voltage-gated sodium and calcium channels (Liebeskind *et al.* 2012), forming a new branch in this super-family. Although the cellular role of the NCA/NALCN channel and how it is gated are not well understood, NALCN and its orthologs are expressed broadly in the nervous system in a number of organisms (Lee *et al.* 1999; Lear *et al.* 2005; Humphrey *et al.* 2007; Lu *et al.* 2007; Jospin *et al.* 2007; Yeh *et al.* 2008; Lu and Feng 2011; Lutas *et al.* 2016). Moreover, mutations in this channel or its auxiliary subunits lead to defects in rhythmic behaviors in multiple organisms (Lear *et al.* 2005; Lu *et al.* 2007; Jospin *et al.* 2007; Yeh *et al.* 2008; Pierce-Shimomura *et al.* 2008; Lear *et al.* 2013; Xie *et al.* 2013; Funato *et al.* 2016). Thus, NCA/NALCN is likely to play an important role in controlling membrane

512 excitability. Additionally, NALCN currents have been reported to be activated by two different G
513 protein-coupled receptors (GPCRs), the muscarinic acetylcholine receptor and the substance P
514 receptor, albeit in a G protein-independent fashion (Lu *et al.* 2009; Swayne *et al.* 2009), and by
515 low extracellular calcium via a G protein-dependent pathway (Lu *et al.* 2010). The latter study
516 further showed that expression of an activated G_q mutant inhibited the NALCN sodium leak
517 current, suggesting that high extracellular calcium tonically inhibits NALCN via a G_q-dependent
518 pathway and that low extracellular calcium activates NALCN by relieving this inhibition (Lu *et al.*
519 2010). By contrast, we find that in *C. elegans*, the physiological role of G_q is to activate NCA-1 and
520 show that NCA-1 is a physiologically relevant target of a G_q signaling pathway that acts through
521 Rho.

522 In the last few years, both recessive and dominant human diseases characterized by a
523 range of neurological symptoms including hypotonia, intellectual disability, and seizures have
524 been shown to be caused by mutations in either *NALCN* or *UNC80* (Köroğlu *et al.* 2013; Al-Sayed
525 *et al.* 2013; Chong *et al.* 2015; Aoyagi *et al.* 2015; Shamseldin *et al.* 2016; Stray-Pedersen *et al.*
526 2016; Gal *et al.* 2016; Fukai *et al.* 2016; Karakaya *et al.* 2016; Perez *et al.* 2016; Bend *et al.* 2016;
527 Wang *et al.* 2016). Notably, dominant disease-causing mutations in the NALCN channel were
528 modeled in worms and resemble either dominant activated or loss-of-function NCA mutants such
529 as the ones we use in this study (Aoyagi *et al.* 2015; Bend *et al.* 2016). Human mutations in other
530 components of the pathway we have described may cause similar clinical phenotypes.

531

532 **Acknowledgments**

533 We thank Shohei Mitani for the *nlf-1(tm3631)* mutant; Steve Nurrish for worm strains and
534 plasmids carrying activated Rho or C3 transferase; Ken Miller for a plasmid with the *unc-17β*
535 promoter; Wayne Davis for FLP/FRT plasmids; Yuji Kohara for cDNA clones; the Sanger Center
536 for cosmids; Brooke Jarvie, Jill Hoyt, and Michelle Giarmarco for the isolation of *unc-79* and *unc-*
537 *80* mutations in the G_q suppressor screen; and Dana Miller for the use of her microscope and

camera to take worm photographs. Some strains were provided by the CGC, which is funded by NIH Office of Research Infrastructure Programs (P40 OD010440). M.A. is an Ellison Medical Foundation New Scholar. E.M.J. is an Investigator of the Howard Hughes Medical Institute. This work was supported by NIH grants R00 MH082109 to M.A and R01 NS034307 to E.M.J.

Figure Legends

Figure 1 Inhibition of Rho in neurons suppresses an activated G_q mutant. (A) Schematic of the FLP/FRT system we used for temporal and spatial expression of the Rho inhibitor C3 transferase (C3T). The transgene in the ‘‘off’’ configuration expresses the mCherry reporter under the control of the promoter sequence but terminates transcription in the *let-858* 3’UTR upstream of GFP-C3T. Expression of the FLP recombinase is induced by heat shock and leads to recombination between the FRT sites and deletion of the intervening *mCherry::let-858* 3’UTR fragment. This leads to transcription of GFP-C3T in the cells driven by the adjacent promoter. We used the pan-neuronal promoter *rab-3p,* acetylcholine neuron promoter *unc-17p,* and head acetylcholine neuron promoter *unc-17Hp.* (B) Inhibition of Rho in adult neurons causes a locomotion defect. Inhibition of Rho by C3 transferase (C3T) in all adult neurons (*rab-3p, oxIs412* transgene), acetylcholine neurons (*unc-17p, oxIs414* transgene) or head acetylcholine neurons (*unc-17Hp, oxIs434* transgene) reduces the locomotion rate of wild type animals. ***, P<0.001, Dunnett’s test. Error bars = SEM; n = 19-20. (C) Inhibition of Rho in all adult neurons (*rab-3p, oxIs412* transgene) or acetylcholine neurons (*unc-17p*, *oxIs414* transgene) led to a significant reduction in the rate of locomotion of the activated G_q mutant *egl-30(tg26)* (here written Gq*). Inhibition of Rho in head acetylcholine neurons (*unc-17Hp*, *oxIs434* transgene) led to a small decrease in Gq* locomotion that was not statistically significant. ***, P<0.001; ns, not significant, P>0.05, Dunnett’s test. Error bars = SEM; n = 10-20. (D) Inhibition of Rho in all adult neurons (*rab-3p*) suppresses the deep body bends of the activated G_q mutant *egl-30(tg26)* (Gq*). Rho inhibition in acetylcholine (*unc-17p*) or head acetylcholine (*unc-17Hp*) neurons did not suppress the waveform of Gq*.

Figure 2 The *nlf-1(ox327)* mutation suppresses the coiled posture and locomotion defect of the activated NCA-1 mutant *nca-1(ox352*) (Nca*). (A) Photos of first-day adult worms. (B) Body bend

assay. (C) Radial locomotion assay. Statistics in B and C: ***, P<0.001, two-tailed Mann-Whitney test. Error bars = SEM, n = 4-8 (panel B), n= 8-26 (panel C).

Figure 3 *nlf-1* mutants are weak fainters. *nlf-1(ox327)* mutant animals have a much weaker fainter phenotype than *unc-80(ox330)* or *nca-2(gk5)*; *nca-1(gk9)* double mutants in the forward direction (A) and a slightly weaker fainter phenotype in the backward direction (B). Additionally, *nlf-1* mutants are enhanced by a mutation in *nca-1*, but not *nca-2*. ***, P<0.001; ns, not significant, P>0.05, Dunn's test. Error bars = SEM; n = 20.

Figure 4 *nlf-1* acts in head acetylcholine neurons to control locomotion. The *nlf-1* cDNA was expressed in an *nlf-1(ox327)* mutant background using the following promoters: *rab-3* (all neurons, *oxEx1146* transgene), *unc-17* (acetylcholine neurons, *oxEx1149* transgene), *unc-17H* (a derivative of the *unc-17* promoter that lacks the enhancer for ventral cord expression and thus expresses only in head acetylcholine neurons, *oxEx1155* transgene), *unc-17β* (a derivative of the *unc-17* promoter that expresses only in ventral cord acetylcholine neurons, *oxEx1323* transgene), *acr-2* (ventral cord acetylcholine motor neurons, *oxEx1151* transgene), and *glr-1* (interneurons including premotor command interneurons, *oxEx1152* transgene). (A) Expression driven by the *rab-3*, *unc-17*, and *unc-17H* promoters rescued the fainting phenotype of an *nlf-1* mutant in the backward direction. ***, P<0.001, Dunn's test. Error bars = SEM; n = 15. (B) Expression driven by the *glr-1* promoter partially rescued the fainting phenotype of an *nlf-1* mutant in either the backward or forward direction, though the effect was not statistically significant (ns, P>0.05, two-tailed Mann-Whitney tests. Error bars = SEM; n = 25). However, assays of this strain were complicated by slow movement and frequent pauses that were hard to distinguish from true fainting behavior (see text for details).

Figure 5 Mutations in NCA channel subunits suppress the high-amplitude waveform of animals expressing activated Rho. Animals expressing an activated Rho mutant (G14V) in acetylcholine neurons (*nzIs29* transgene, written as Rho*) have a high-amplitude waveform. Mutations that eliminate NCA-1 and NCA-2 channel function (*unc-80(ox330)* or *nca-2(gk5)*; *nca-1(gk9)*) strongly suppress the high-amplitude waveform of activated Rho and convert the activated Rho mutants to fainters. Mutations in *nlf-1(ox327)* and *nca-1(gk9)* strongly but incompletely suppress the high-amplitude waveform of activated Rho and these double mutants do not faint. Mutations in *nca-2(gk5)* do not suppress the high-amplitude waveform of activated Rho. Mutants in *unc-80*, *nlf-1*, and the *nca-2 nca-1* double mutant have the typical fainter posture characterized by a straightened anterior part of the body.

Figure 6 Mutations in *nlf-1* and *nca-1* suppress the locomotion defect of animals expressing activated Rho. Animals expressing an activated Rho mutant (G14V) in acetylcholine neurons (*nzIs29* transgene, written as Rho*) have a slow locomotion rate. The *nlf-1(ox327)* and *nca-1(gk9)* mutations, but not *nca-2(gk5)*, strongly suppress the slow locomotion rate of activated Rho. ***, P<0.001, Bonferroni test. Error bars = SEM; n = 16.

Figure 7 Model. G_q activates NCA-1 in a linear pathway via the RhoGEF Trio and small G protein Rho. G_q activation of Trio and Rho is direct (solid arrow). Rho activation of NCA-1 is likely to be indirect (dashed arrow). G_o inhibits G_q via the RGS protein EAT-16 (not shown). Thus, loss-of-function mutations in NCA-1, its associated subunits UNC-79 and UNC-80, or the ER-localized assembly factor NLF-1 suppress an activated G_q mutant, whereas a gain-of-function activating mutation in NCA-1 suppresses an activated G_o mutant.

Figure S1 Mutations affecting the NCA-1 channel suppress the high-amplitude waveform of the activated G_q mutant *egl-30(tg26)* (Gq*). The *unc-79(yak37)* and *unc-80(ox330)* mutations strongly

suppress the high-amplitude waveform of Gq*. The *nca-1(gk9)* and *nlf-1(ox327)* mutations partially suppress the high-amplitude waveform of Gq*. Mutations in genes required for dense-core vesicle biogenesis such as *rund-1(tm3622)* or the canonical G_q pathway such as *egl-8(ox333)* only weakly suppress the high-amplitude waveform of Gq*. The *nca-2(gk5)* mutation does not suppress Gq*.

Figure S2 *nlf-1* mutants have reduced *nca-1::gfp* and *nca-2::gfp* fluorescence in the nerve ring. Quantification of the nerve ring fluorescence of C-terminally tagged *nca-1::gfp* (transgene *vaIs46*) and *nca-2::gfp* (transgene *vaIs41*) in wild type and *nlf-1(ox327)* mutants. ***, P<0.001, two-tailed unpaired t tests where each mutant strain is compared to its associated wild-type control. Error bars = SEM; n = 11-12.

Figure S3 *nlf-1* is expressed widely in the nervous system. A fusion of the *nlf-1* promoter to GFP (transgene *oxEx1144*) is expressed throughout the nervous system, including head and tail neurons, and motor neurons in the ventral nerve cord. No expression is seen in non-neuronal tissues. An L1 stage larval animal is shown with its head to the left.

Figure S4 Mutations in NCA channel subunits suppress the locomotion defect of animals expressing activated Rho. Animals expressing an activated Rho mutant (G14V) in acetylcholine neurons (*nzIs29* transgene, written as Rho*) have reduced locomotion as measured in radial locomotion assays. Mutations that eliminate function of the NCA channels (*unc-80(ox330)* or *nca-2(gk5);nca-1(gk9)*) increase the radial distance traveled by activated Rho mutants, but the effect is subtle since *unc-80* and *nca-2; nca-1* mutants have reduced locomotion on their own. The *nlf-1(ox327)* mutation that partially but incompletely reduces function of the NCA channels strongly suppresses the locomotion defect of activated Rho. ***, P<0.0001, Bonferroni test. Error bars = SEM; n = 5-18.

Figure S5 Mutations in NCA channel subunits suppress the high-amplitude waveform and locomotion of adult animals expressing activated Rho. (A) Animals expressing an activated Rho mutant (G14V) only in adults by heat-shock induced expression (*nzIs1* transgene, *hs::Rho**) have a high-amplitude waveform. The *unc-80(ox330)* and *nlf-1(ox327)* mutations strongly suppress the high-amplitude waveform of activated Rho. *unc-80*, but not *nlf-1*, makes the activated Rho animals faint. (B) Animals expressing an activated Rho mutant (G14V) only in adults by heat-shock induced expression (*nzIs1* transgene, *hs::Rho**) have a reduced locomotion rate. The *nlf-1(ox327)* mutation suppresses the reduced locomotion rate of activated Rho. *, P=0.0157, two-tailed unpaired t test. Error bars = SEM; n = 18-30)

Literature Cited

Adachi T., Kunitomo H., Tomioka M., Ohno H., Okochi Y., Mori I., Iino Y., 2010 Reversal of salt preference is directed by the insulin/PI3K and Gq/PKC signaling in Caenorhabditis elegans. Genetics **186**: 1309–1319.

Ailion M., Hannemann M., Dalton S., Pappas A., Watanabe S., Hegermann J., Liu Q., Han H.-F., Gu M., Goulding M. Q., Sasidharan N., Schuske K., Hullett P., Eimer S., Jorgensen E. M., 2014 Two Rab2 interactors regulate dense-core vesicle maturation. Neuron **82**: 167–180.

Al-Sayed M. D., Al-Zaidan H., Albakheet A., Hakami H., Kenana R., Al-Yafee Y., Al-Dosary M., Qari A., Al-Sheddi T., Al-Muheiza M., Al-Qubbaj W., Lakmache Y., Al-Hindi H., Ghaziuddin M., Colak D., Kaya N., 2013 Mutations in NALCN cause an autosomal-recessive syndrome with severe hypotonia, speech impairment, and cognitive delay. Am. J. Hum. Genet. **93**: 721–726.

Aoyagi K., Rossignol E., Hamdan F. F., Mulcahy B., Xie L., Nagamatsu S., Rouleau G. A., Zhen M., Michaud J. L., 2015 A Gain-of-Function Mutation in NALCN in a Child with Intellectual Disability, Ataxia, and Arthrogryposis. Hum. Mutat. **36**: 753–757.

Balla T., 2013 Phosphoinositides: tiny lipids with giant impact on cell regulation. Physiol. Rev. **93**: 1019–1137.

Bastiani C. A., Gharib S., Simon M. I., Sternberg P. W., 2003 Caenorhabditis elegans Galphaq regulates egg-laying behavior via a PLCbeta-independent and serotonin-dependent signaling pathway and likely functions both in the nervous system and in muscle. Genetics **165**: 1805–1822.

Bend E. G., Si Y., Stevenson D. A., Bayrak-Toydemir P., Newcomb T. M., Jorgensen E. M., Swoboda K. J., 2016 NALCN channelopathies: Distinguishing gain-of-function and loss-of-function mutations. Neurology **87**: 1131–1139.

Boone A. N., Senatore A., Chemin J., Monteil A., Spafford J. D., 2014 Gd3+ and calcium sensitive, sodium leak currents are features of weak membrane-glass seals in patch clamp recordings. PLoS ONE **9**: e98808.

Brundage L., Avery L., Katz A., Kim U. J., Mendel J. E., Sternberg P. W., Simon M. I., 1996 Mutations in a C. elegans Gqalpha gene disrupt movement, egg laying, and viability. Neuron **16**: 999–1009.

Charlie N. K., Schade M. A., Thomure A. M., Miller K. G., 2006 Presynaptic UNC-31 (CAPS) is required to activate the G alpha(s) pathway of the Caenorhabditis elegans synaptic signaling network. Genetics **172**: 943–961.

Chatah N. E., Abrams C. S., 2001 G-protein-coupled receptor activation induces the membrane translocation and activation of phosphatidylinositol-4-phosphate 5-kinase I alpha by a Rac- and Rho-dependent pathway. J. Biol. Chem. **276**: 34059–34065.

Chong J. X., McMillin M. J., Shively K. M., Beck A. E., Marvin C. T., Armenteros J. R., Buckingham K. J., Nkinsi N. T., Boyle E. A., Berry M. N., Bocian M., Foulds N., Uzielli M. L. G., Haldeman-Englert C., Hennekam R. C. M., Kaplan P., Kline A. D., Mercer C. L., Nowaczyk M. J. M., Klein Wassink-Ruiter J. S., McPherson E. W., Moreno R. A., Scheuerle A. E., Shashi V., Stevens C. A., Carey J. C., Monteil A., Lory P., Tabor H. K., Smith J. D., Shendure J., Nickerson D. A., University of Washington Center for Mendelian Genomics, Bamshad M. J., 2015 De novo mutations in NALCN cause a syndrome characterized by congenital contractures of the limbs and face, hypotonia, and developmental delay. Am. J. Hum. Genet. **96**: 462–473.

Coleman D. E., Berghuis A. M., Lee E., Linder M. E., Gilman A. G., Sprang S. R., 1994 Structures of active conformations of Gi alpha 1 and the mechanism of GTP hydrolysis. Science **265**: 1405–1412.

Coulon P., Kanyshkova T., Broicher T., Munsch T., Wettschureck N., Seidenbecher T., Meuth S. G., Offermanns S., Pape H.-C., Budde T., 2010 Activity Modes in Thalamocortical Relay Neurons are Modulated by G(q)/G(11) Family G-proteins - Serotonergic and Glutamatergic Signaling. Front Cell Neurosci **4**: 132.

Davis M. W., Hammarlund M., Harrach T., Hullett P., Olsen S., Jorgensen E. M., 2005 Rapid single nucleotide polymorphism mapping in C. elegans. BMC Genomics **6**: 118.

705 Davis M. W., Morton J. J., Carroll D., Jorgensen E. M., 2008 Gene activation using FLP recombinase in C.
706 elegans. PLoS Genet. **4**: e1000028.

707 Esposito G., Amoroso M. R., Bergamasco C., Di Schiavi E., Bazzicalupo P., 2010 The G protein regulators
708 EGL-10 and EAT-16, the Giα GOA-1 and the G(q)α EGL-30 modulate the response of the C.
709 elegans ASH polymodal nociceptive sensory neurons to repellents. BMC Biol. **8**: 138.

710 Etienne-Manneville S., Hall A., 2002 Rho GTPases in cell biology. Nature **420**: 629–635.

711 Fukai R., Saitsu H., Okamoto N., Sakai Y., Fattal-Valevski A., Masaaki S., Kitai Y., Torio M., Kojima-Ishii
712 K., Ihara K., Chernuha V., Nakashima M., Miyatake S., Tanaka F., Miyake N., Matsumoto N., 2016
713 De novo missense mutations in NALCN cause developmental and intellectual impairment with
714 hypotonia. J. Hum. Genet. **61**: 451–455.

715 Funato H., Miyoshi C., Fujiyama T., Kanda T., Sato M., Wang Z., Ma J., Nakane S., Tomita J., Ikkyu A.,
716 Kakizaki M., Hotta-Hirashima N., Kanno S., Komiya H., Asano F., Honda T., Kim S. J., Harano K.,
717 Muramoto H., Yonezawa T., Mizuno S., Miyazaki S., Connor L., Kumar V., Miura I., Suzuki T.,
718 Watanabe A., Abe M., Sugiyama F., Takahashi S., Sakimura K., Hayashi Y., Liu Q., Kume K.,
719 Wakana S., Takahashi J. S., Yanagisawa M., 2016 Forward-genetics analysis of sleep in randomly
720 mutagenized mice. Nature **539**: 378–383.

721 Gal M., Magen D., Zahran Y., Ravid S., Eran A., Khayat M., Gafni C., Levanon E. Y., Mandel H., 2016 A
722 novel homozygous splice site mutation in NALCN identified in siblings with cachexia, strabismus,
723 severe intellectual disability, epilepsy and abnormal respiratory rhythm. Eur J Med Genet **59**: 204–
724 209.

725 Gamper N., Reznikov V., Yamada Y., Yang J., Shapiro M. S., 2004 Phosphatidylinositol [correction] 4,5-
726 bisphosphate signals underlie receptor-specific Gq/11-mediated modulation of N-type Ca2+
727 channels. J. Neurosci. **24**: 10980–10992.

728 Gao S., Xie L., Kawano T., Po M. D., Pirri J. K., Guan S., Alkema M. J., Zhen M., 2015 The NCA sodium
729 leak channel is required for persistent motor circuit activity that sustains locomotion. Nat Commun
730 **6**: 6323.

731 Hajdu-Cronin Y. M., Chen W. J., Patikoglou G., Koelle M. R., Sternberg P. W., 1999 Antagonism between
732 G(o)alpha and G(q)alpha in Caenorhabditis elegans: the RGS protein EAT-16 is necessary for
733 G(o)alpha signaling and regulates G(q)alpha activity. Genes Dev **13**: 1780–1793.

734 Hajdu-Cronin Y. M., Chen W. J., Sternberg P. W., 2004 The L-type cyclin CYL-1 and the heat-shock-factor
735 HSF-1 are required for heat-shock-induced protein expression in Caenorhabditis elegans. Genetics
736 **168**: 1937–1949.

737 Hammarlund M., Palfreyman M. T., Watanabe S., Olsen S., Jorgensen E. M., 2007 Open syntaxin docks
738 synaptic vesicles. PLoS Biol. **5**: e198.

739 Hiley E., McMullan R., Nurrish S. J., 2006 The Galpha12-RGS RhoGEF-RhoA signalling pathway regulates
740 neurotransmitter release in C. elegans. EMBO J. **25**: 5884–5895.

741 Humphrey J. A., Hamming K. S., Thacker C. M., Scott R. L., Sedensky M. M., Snutch T. P., Morgan P. G.,
742 Nash H. A., 2007 A putative cation channel and its novel regulator: cross-species conservation of
743 effects on general anesthesia. Curr. Biol. **17**: 624–629.

744 Jaffe A. B., Hall A., 2005 Rho GTPases: biochemistry and biology. Annu. Rev. Cell Dev. Biol. **21**: 247–269.

745 Jantsch-Plunger V., Gönczy P., Romano A., Schnabel H., Hamill D., Schnabel R., Hyman A. A., Glotzer M.,
746 2000 CYK-4: A Rho family gtpase activating protein (GAP) required for central spindle formation
747 and cytokinesis. J. Cell Biol. **149**: 1391–1404.

748 Jospin M., Watanabe S., Joshi D., Young S., Hamming K., Thacker C., Snutch T. P., Jorgensen E. M.,
749 Schuske K., 2007 UNC-80 and the NCA ion channels contribute to endocytosis defects in
750 synaptojanin mutants. Curr. Biol. **17**: 1595–1600.

751 Karakaya M., Heller R., Kunde V., Zimmer K.-P., Chao C.-M., Nürnberg P., Cirak S., 2016 Novel Mutations
752 in the Nonselective Sodium Leak Channel (NALCN) Lead to Distal Arthrogryposis with Increased
753 Muscle Tone. Neuropediatrics **47**:273-277.

754 Köroğlu Ç., Seven M., Tolun A., 2013 Recessive truncating NALCN mutation in infantile neuroaxonal
755 dystrophy with facial dysmorphism. J. Med. Genet. **50**: 515–520.

756 Krause M., Offermanns S., Stocker M., Pedarzani P., 2002 Functional specificity of G alpha q and G alpha
757 11 in the cholinergic and glutamatergic modulation of potassium currents and excitability in
758 hippocampal neurons. J. Neurosci. **22**: 666–673.

759 Lackner M. R., Nurrish S. J., Kaplan J. M., 1999 Facilitation of synaptic transmission by EGL-30 Gqalpha
760 and EGL-8 PLCbeta: DAG binding to UNC-13 is required to stimulate acetylcholine release. Neuron
761 **24**: 335–346.

762 Lear B. C., Lin J.-M., Keath J. R., McGill J. J., Raman I. M., Allada R., 2005 The ion channel narrow
763 abdomen is critical for neural output of the Drosophila circadian pacemaker. Neuron **48**: 965–976.

764 Lear B. C., Darrah E. J., Aldrich B. T., Gebre S., Scott R. L., Nash H. A., Allada R., 2013 UNC79 and
765 UNC80, Putative Auxiliary Subunits of the NARROW ABDOMEN Ion Channel, Are Indispensable
766 for Robust Circadian Locomotor Rhythms in Drosophila. PLoS ONE **8**: e78147.

767 Lee J. H., Cribbs L. L., Perez-Reyes E., 1999 Cloning of a novel four repeat protein related to voltage-
768 gated sodium and calcium channels. FEBS Lett. **445**: 231–236.

769 Liebeskind B. J., Hillis D. M., Zakon H. H., 2012 Phylogeny unites animal sodium leak channels with fungal
770 calcium channels in an ancient, voltage-insensitive clade. Mol. Biol. Evol. **29**: 3613–3616.

771 Littleton J. T., Ganetzky B., 2000 Ion channels and synaptic organization: analysis of the Drosophila
772 genome. Neuron **26**: 35–43.

773 Lu B., Su Y., Das S., Liu J., Xia J., Ren D., 2007 The neuronal channel NALCN contributes resting sodium
774 permeability and is required for normal respiratory rhythm. Cell **129**: 371–383.

775 Lu B., Su Y., Das S., Wang H., Wang Y., Liu J., Ren D., 2009 Peptide neurotransmitters activate a cation
776 channel complex of NALCN and UNC-80. Nature **457**: 741–744.

777 Lu B., Zhang Q., Wang H., Wang Y., Nakayama M., Ren D., 2010 Extracellular calcium controls
778 background current and neuronal excitability via an UNC79-UNC80-NALCN cation channel
779 complex. Neuron **68**: 488–499.

780 Lu T. Z., Feng Z.-P., 2011 A sodium leak current regulates pacemaker activity of adult central pattern
781 generator neurons in Lymnaea stagnalis. PLoS ONE **6**: e18745.

782 Lutas A., Lahmann C., Soumillon M., Yellen G., 2016 The leak channel NALCN controls tonic firing and
783 glycolytic sensitivity of substantia nigra pars reticulata neurons. eLife **5**: e15271.

784 Lutz S., Freichel-Blomquist A., Yang Y., Rümenapp U., Jakobs K. H., Schmidt M., Wieland T., 2005 The
785 guanine nucleotide exchange factor p63RhoGEF, a specific link between Gq/11-coupled receptor
786 signaling and RhoA. J. Biol. Chem. **280**: 11134–11139.

787 Lutz S., Shankaranarayanan A., Coco C., Ridilla M., Nance M. R., Vettel C., Baltus D., Evelyn C. R.,
788 Neubig R. R., Wieland T., Tesmer J. J. G., 2007 Structure of Galphaq-p63RhoGEF-RhoA complex
789 reveals a pathway for the activation of RhoA by GPCRs. Science **318**: 1923–1927.

790 Matsuki M., Kunitomo H., Iino Y., 2006 Goalpha regulates olfactory adaptation by antagonizing Gqalpha-
791 DAG signaling in Caenorhabditis elegans. Proc. Natl. Acad. Sci. U.S.A. **103**: 1112–1117.

792 McMullan R., Hiley E., Morrison P., Nurrish S. J., 2006 Rho is a presynaptic activator of neurotransmitter
793 release at pre-existing synapses in C. elegans. Genes Dev. **20**: 65–76.

794 Mello C. C., Kramer J. M., Stinchcomb D., Ambros V., 1991 Efficient gene transfer in C.elegans:
795 extrachromosomal maintenance and integration of transforming sequences. EMBO J **10**: 3959–
796 3970.

797 Miller K. G., Emerson M. D., Rand J. B., 1999 Goalpha and diacylglycerol kinase negatively regulate the
798 Gqalpha pathway in C. elegans. Neuron **24**: 323–333.

799 Park E. C., Horvitz H. R., 1986 Mutations with dominant effects on the behavior and morphology of the
800 nematode Caenorhabditis elegans. Genetics **113**: 821–852.

801 Pereira L., Kratsios P., Serrano-Saiz E., Sheftel H., Mayo A. E., Hall D. H., White J. G., LeBoeuf B., Garcia
802 L. R., Alon U., Hobert O., 2015 A cellular and regulatory map of the cholinergic nervous system of
803 C. elegans. eLife **4**: e12432.

804 Perez Y., Kadir R., Volodarsky M., Noyman I., Flusser H., Shorer Z., Gradstein L., Birnbaum R. Y., Birk O.
805 S., 2016 UNC80 mutation causes a syndrome of hypotonia, severe intellectual disability, dyskinesia
806 and dysmorphism, similar to that caused by mutations in its interacting cation channel NALCN. J.
807 Med. Genet. **53**: 397–402.

808 Pierce-Shimomura J. T., Chen B. L., Mun J. J., Ho R., Sarkis R., McIntire S. L., 2008 Genetic analysis of
809 crawling and swimming locomotory patterns in C. elegans. Proc. Natl. Acad. Sci. U.S.A. **105**:
810 20982–20987.

811 Sánchez-Fernández G., Cabezudo S., García-Hoz C., Benincá C., Aragay A. M., Mayor F., Ribas C., 2014
812 Gαq signalling: the new and the old. Cell. Signal. **26**: 833–848.

813 Senatore A., Monteil A., Minnen J. van, Smit A. B., Spafford J. D., 2013 NALCN ion channels have
814 alternative selectivity filters resembling calcium channels or sodium channels. PLoS ONE **8**:
815 e55088.

816 Senatore A., Spafford J. D., 2013 A uniquely adaptable pore is consistent with NALCN being an ion sensor.
817 Channels (Austin) **7**: 60–68.

818 Shamseldin H. E., Faqeih E., Alasmari A., Zaki M. S., Gleeson J. G., Alkuraya F. S., 2016 Mutations in
819 UNC80, Encoding Part of the UNC79-UNC80-NALCN Channel Complex, Cause Autosomal-
820 Recessive Severe Infantile Encephalopathy. Am. J. Hum. Genet. **98**: 210–215.

821 Stray-Pedersen A., Cobben J.-M., Prescott T. E., Lee S., Cang C., Aranda K., Ahmed S., Alders M.,
822 Gerstner T., Aslaksen K., Tétreault M., Qin W., Hartley T., Jhangiani S. N., Muzny D. M., Tarailo-

Graovac M., Karnebeek C. D. M. van, Care4Rare Canada Consortium, Baylor-Hopkins Center for Mendelian Genomics, Lupski J. R., Ren D., Yoon G., 2016 Biallelic Mutations in UNC80 Cause Persistent Hypotonia, Encephalopathy, Growth Retardation, and Severe Intellectual Disability. Am. J. Hum. Genet. **98**: 202–209.

Swayne L. A., Mezghrani A., Varrault A., Chemin J., Bertrand G., Dalle S., Bourinet E., Lory P., Miller R. J., Nargeot J., Monteil A., 2009 The NALCN ion channel is activated by M3 muscarinic receptors in a pancreatic beta-cell line. EMBO Rep. **10**: 873–880.

Topalidou I., Cattin-Ortolá J., Pappas A. L., Cooper K., Merrihew G. E., MacCoss M. J., Ailion M., 2016 The EARP Complex and Its Interactor EIPR-1 Are Required for Cargo Sorting to Dense-Core Vesicles. PLoS Genet. **12**: e1006074.

Vogt S., Grosse R., Schultz G., Offermanns S., 2003 Receptor-dependent RhoA activation in G12/G13-deficient cells: genetic evidence for an involvement of Gq/G11. J. Biol. Chem. **278**: 28743–28749.

Wang Y., Koh K., Ichinose Y., Yasumura M., Ohtsuka T., Takiyama Y., 2016 A de novo mutation in the NALCN gene in an adult patient with cerebellar ataxia associated with intellectual disability and arthrogryposis. Clin. Genet. **90**: 556–557.

Weernink P. A. O., Meletiadis K., Hommeltenberg S., Hinz M., Ishihara H., Schmidt M., Jakobs K. H., 2004 Activation of type I phosphatidylinositol 4-phosphate 5-kinase isoforms by the Rho GTPases, RhoA, Rac1, and Cdc42. J. Biol. Chem. **279**: 7840–7849.

Wilkie T. M., Scherle P. A., Strathmann M. P., Slepak V. Z., Simon M. I., 1991 Characterization of G-protein alpha subunits in the Gq class: expression in murine tissues and in stromal and hematopoietic cell lines. Proc. Natl. Acad. Sci. U.S.A. **88**: 10049–10053.

Wilkie T. M., Gilbert D. J., Olsen A. S., Chen X. N., Amatruda T. T., Korenberg J. R., Trask B. J., Jong P. de, Reed R. R., Simon M. I., 1992 Evolution of the mammalian G protein alpha subunit multigene family. Nat. Genet. **1**: 85–91.

847 Williams S. L., Lutz S., Charlie N. K., Vettel C., Ailion M., Coco C., Tesmer J. J. G., Jorgensen E. M.,
848 Wieland T., Miller K. G., 2007 Trio's Rho-specific GEF domain is the missing Galpha q effector in C.
849 elegans. Genes Dev **21**: 2731–2746.

850 Xie L., Gao S., Alcaire S. M., Aoyagi K., Wang Y., Griffin J. K., Stagljar I., Nagamatsu S., Zhen M., 2013
851 NLF-1 delivers a sodium leak channel to regulate neuronal excitability and modulate rhythmic
852 locomotion. Neuron **77**: 1069–1082.

853 Yeh E., Ng S., Zhang M., Bouhours M., Wang Y., Wang M., Hung W., Aoyagi K., Melnik-Martinez K., Li M.,
854 Liu F., Schafer W. R., Zhen M., 2008 A putative cation channel, NCA-1, and a novel protein, UNC-
855 80, transmit neuronal activity in C. elegans. PLoS Biol. **6**: e55.

856

Figure 1

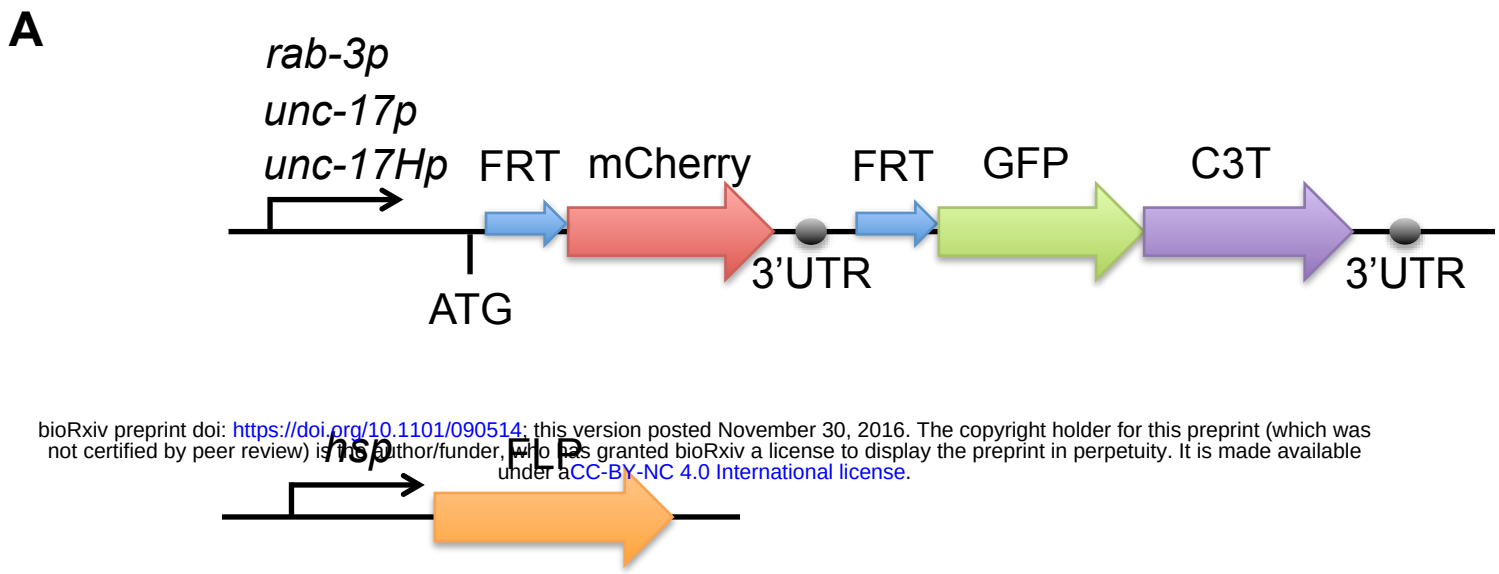

Figure 2

Figure 3

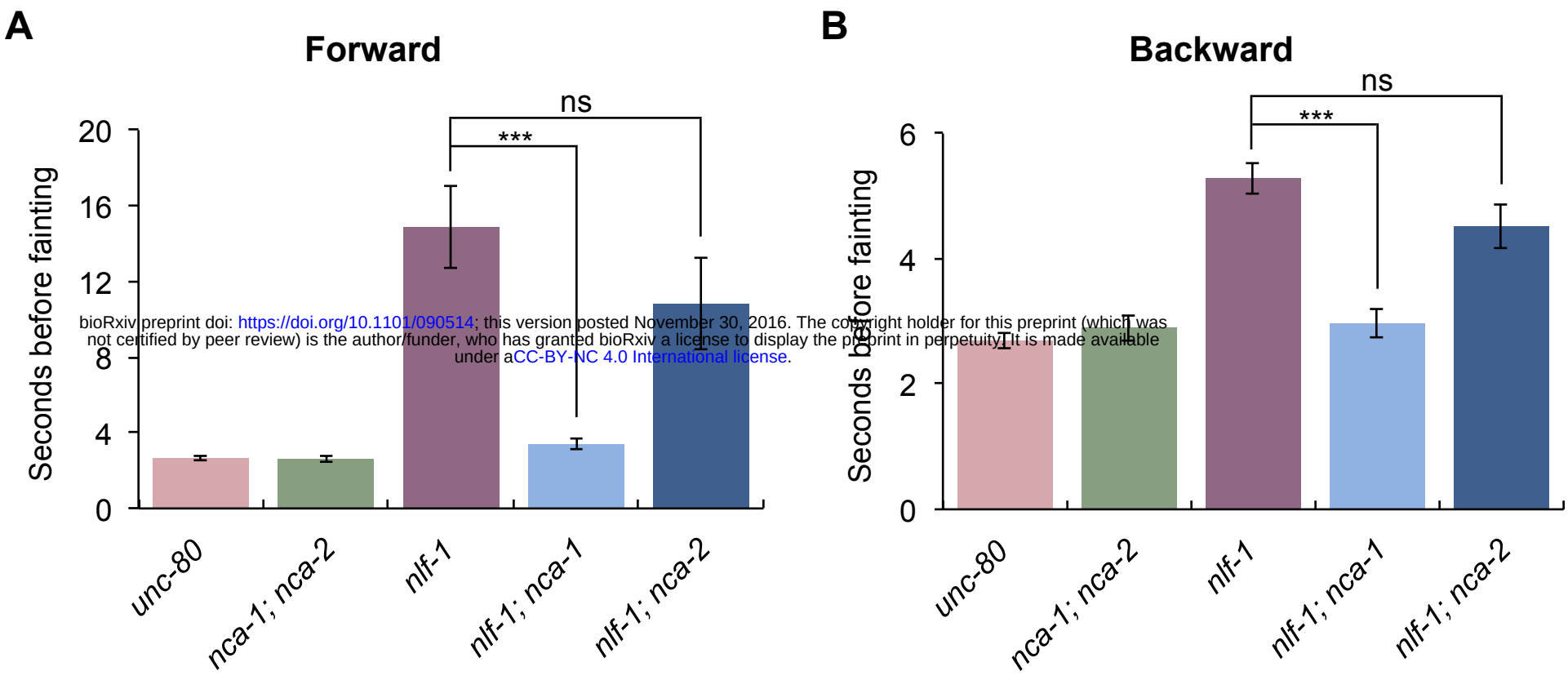

Figure 4

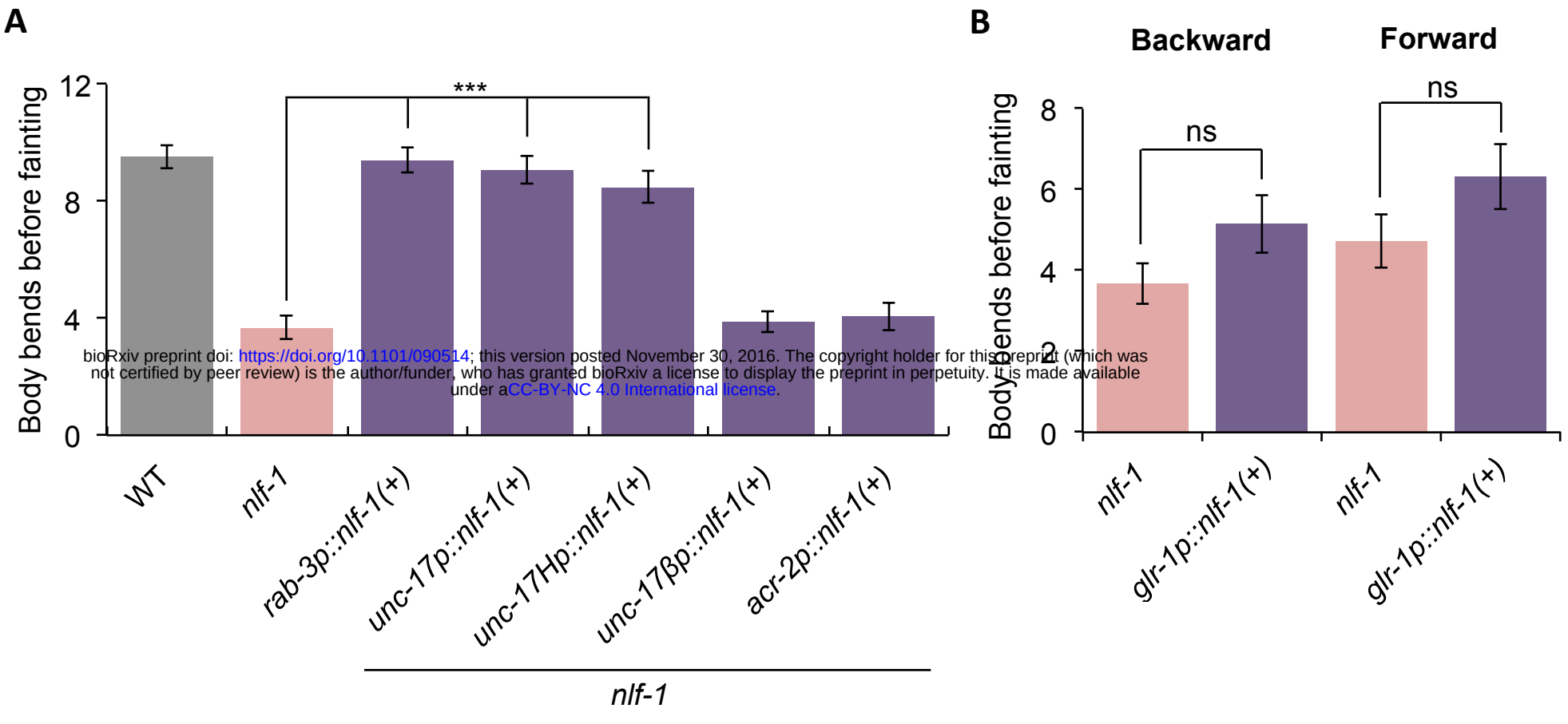

Figure 5

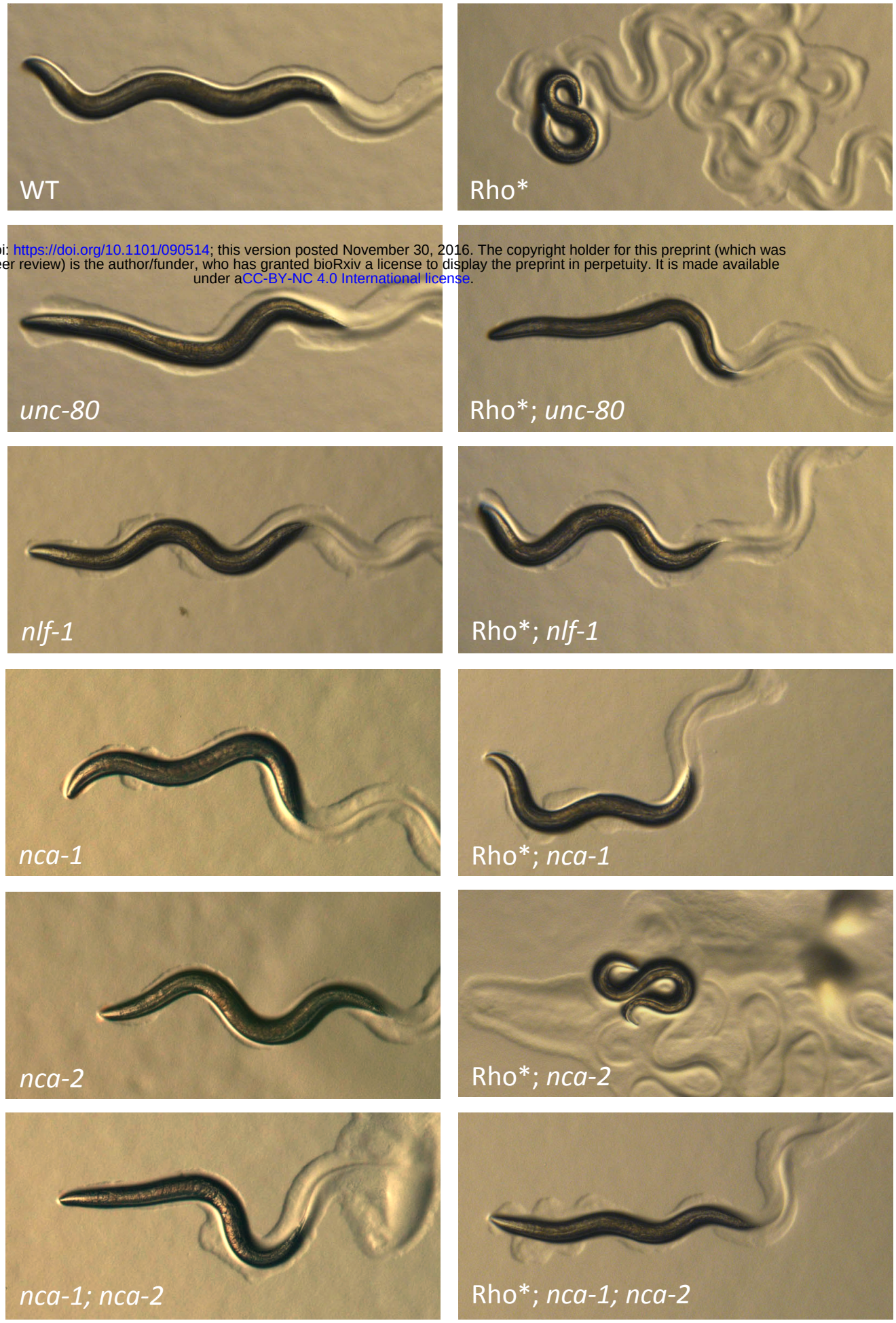

Figure 6

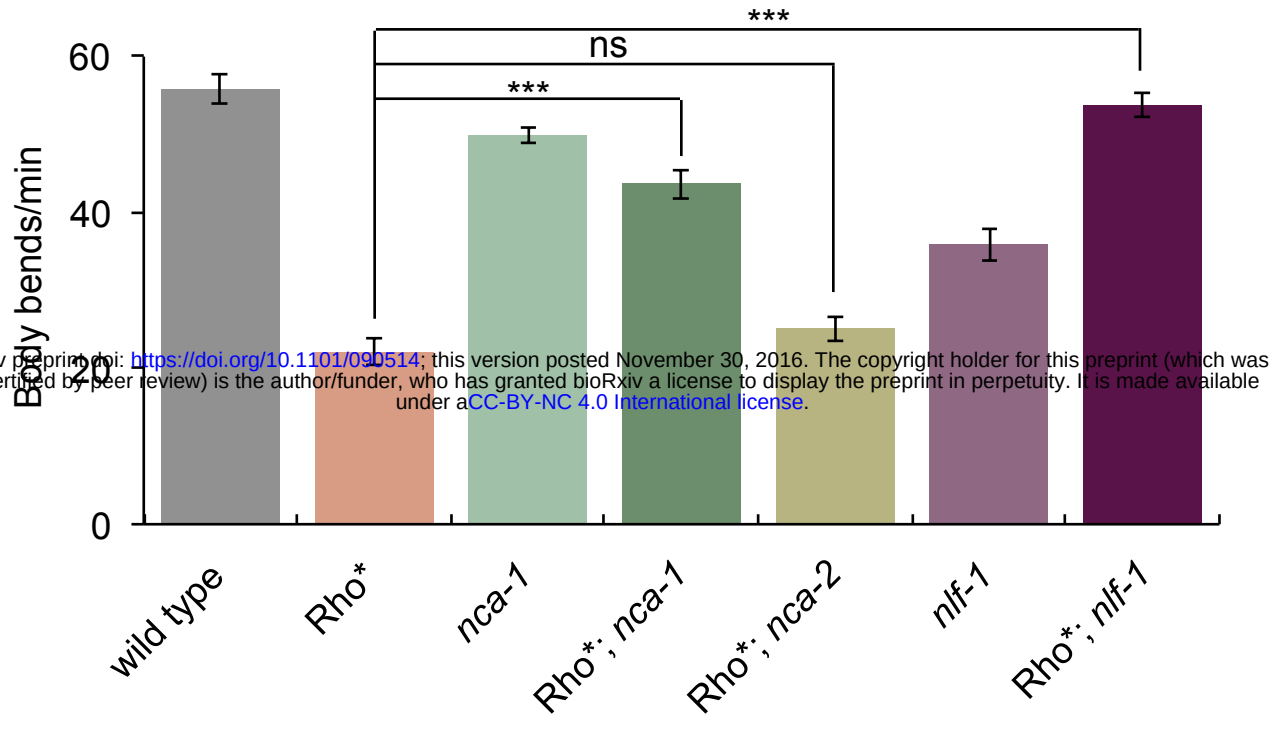

Figure 7

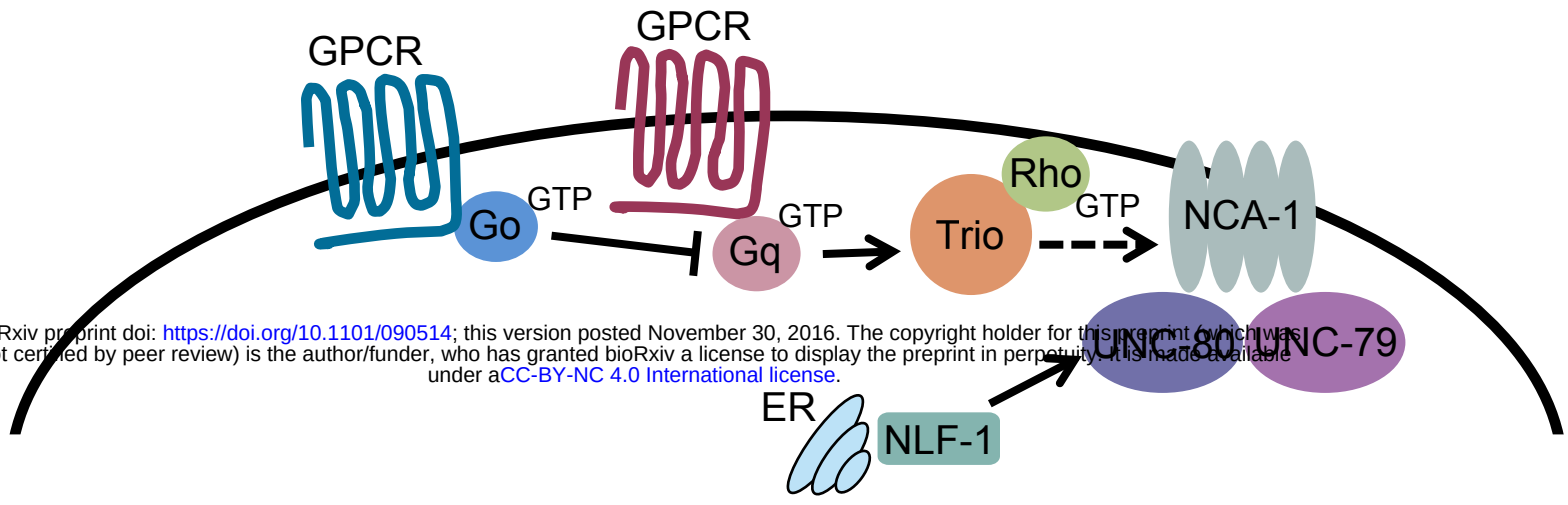

Figure S1

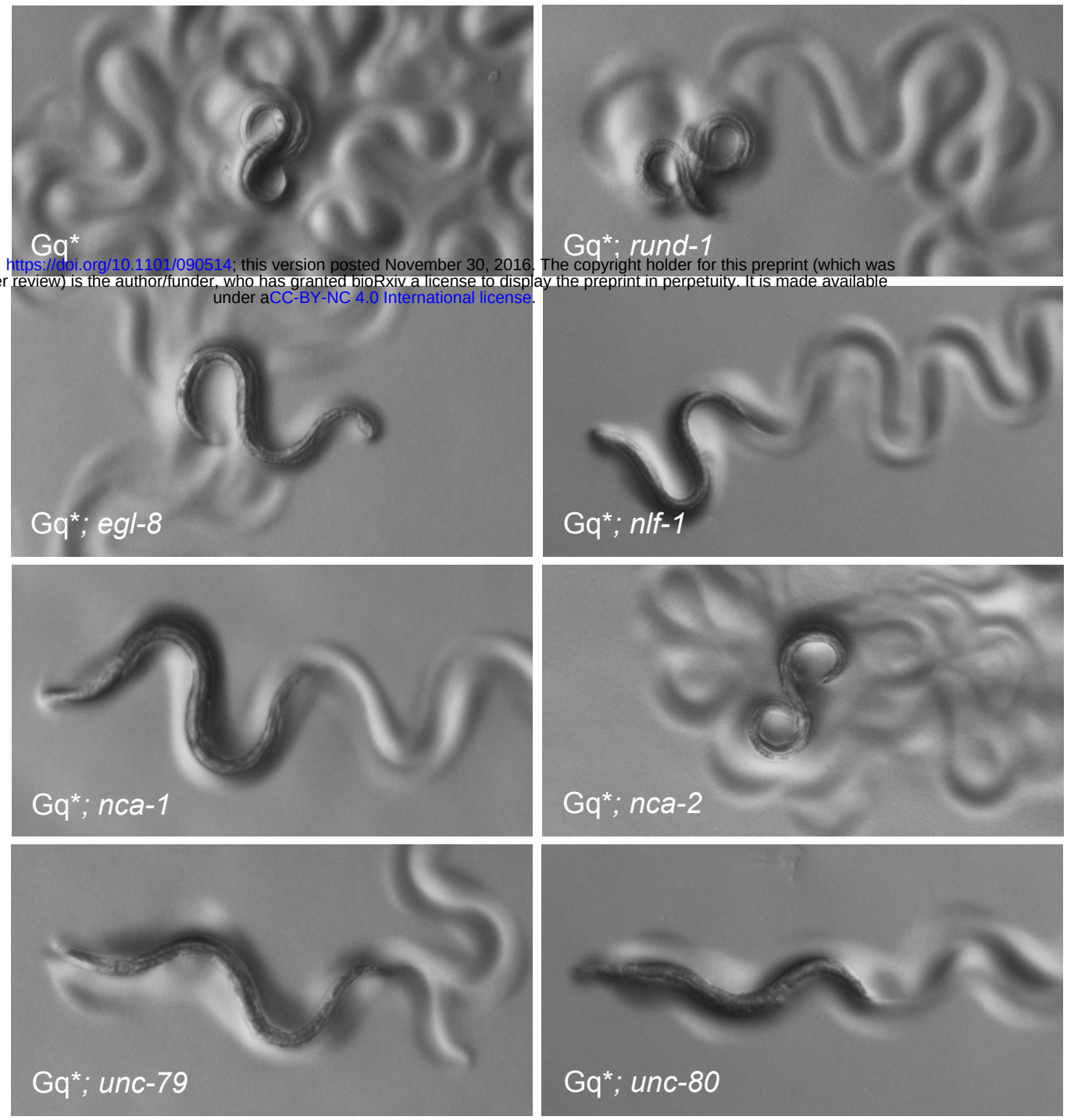

Figure S2

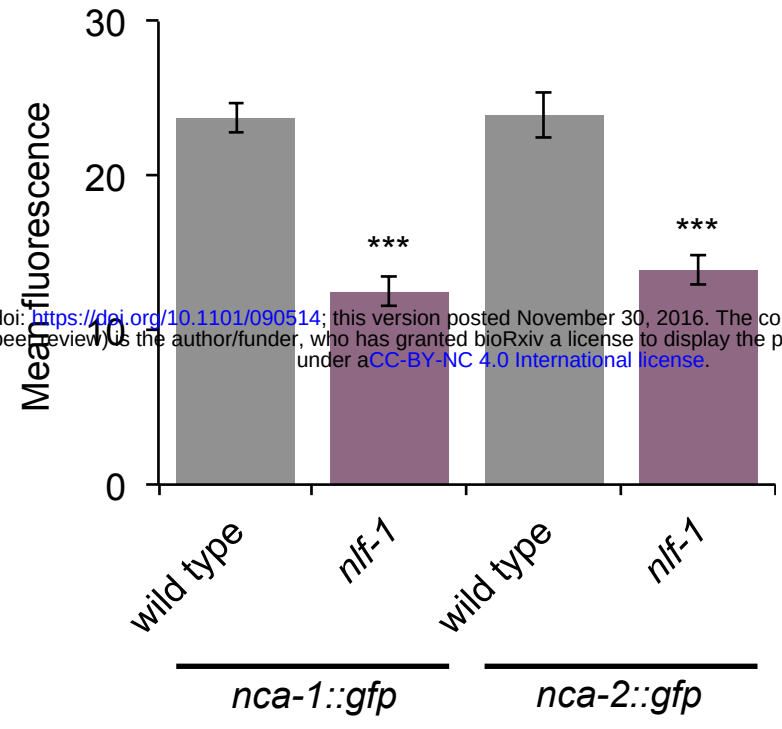

Figure S3

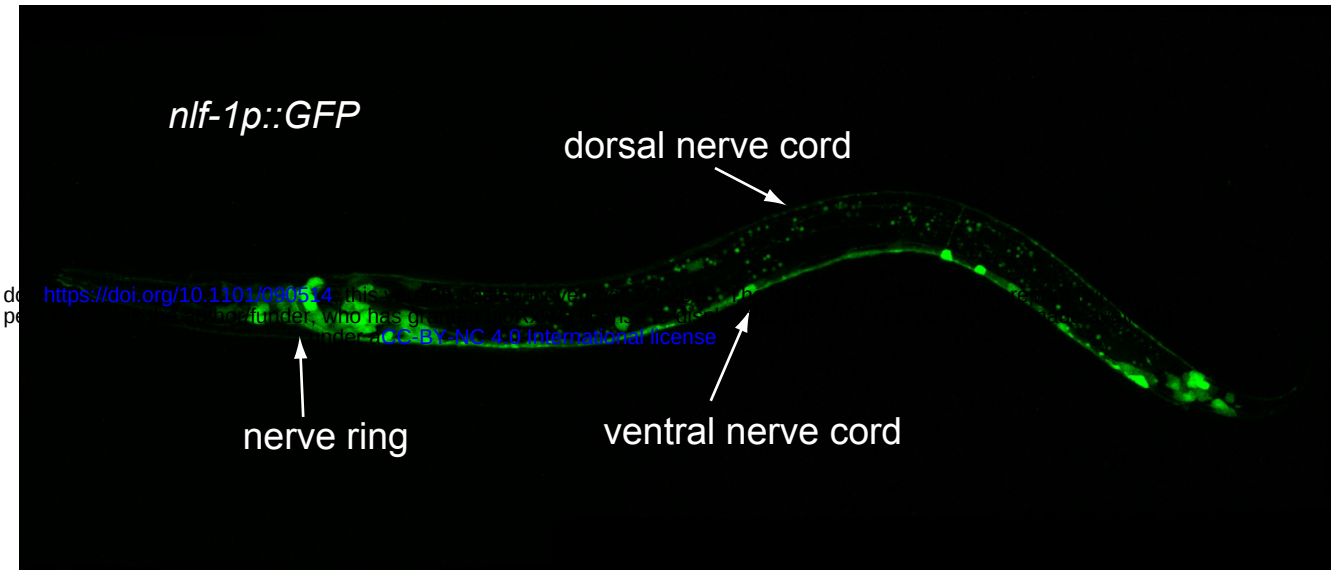

Figure S4

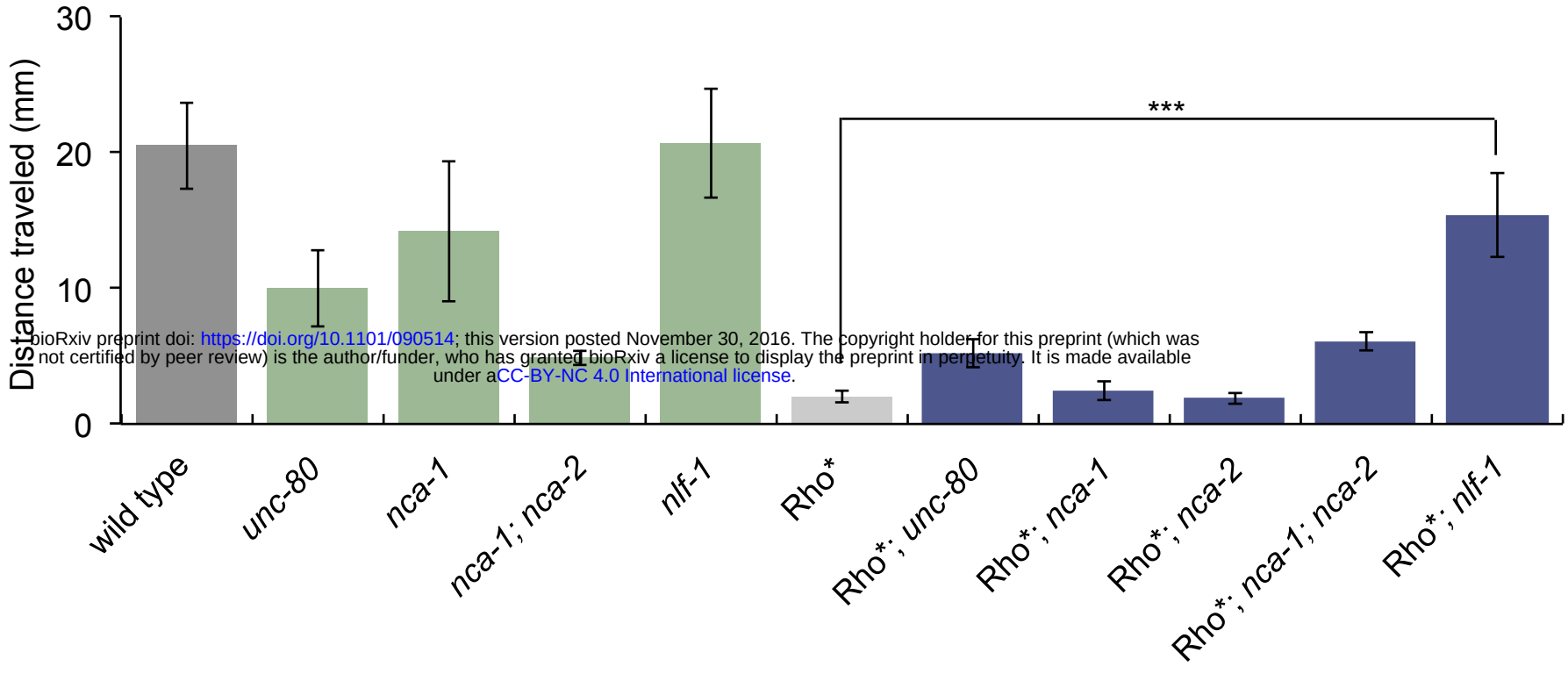

Figure S5

A

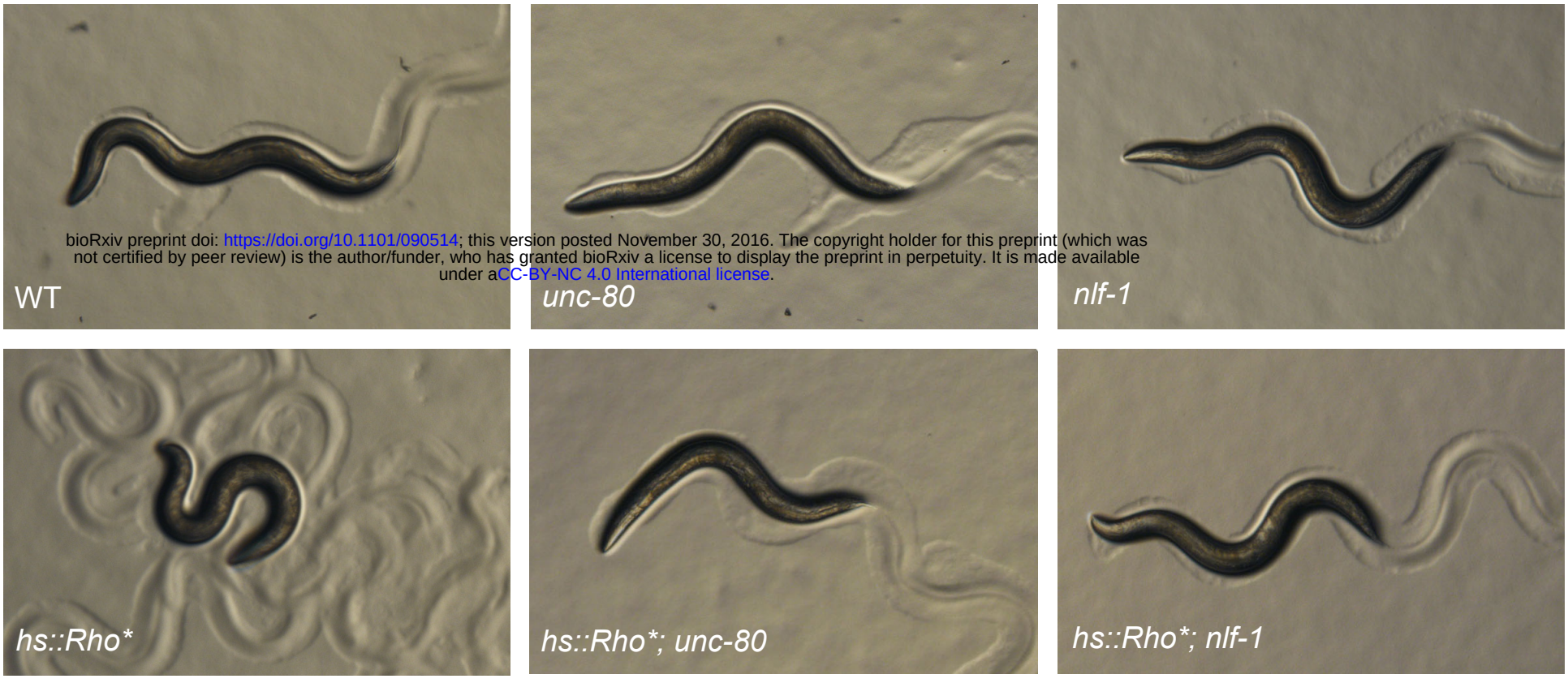

B

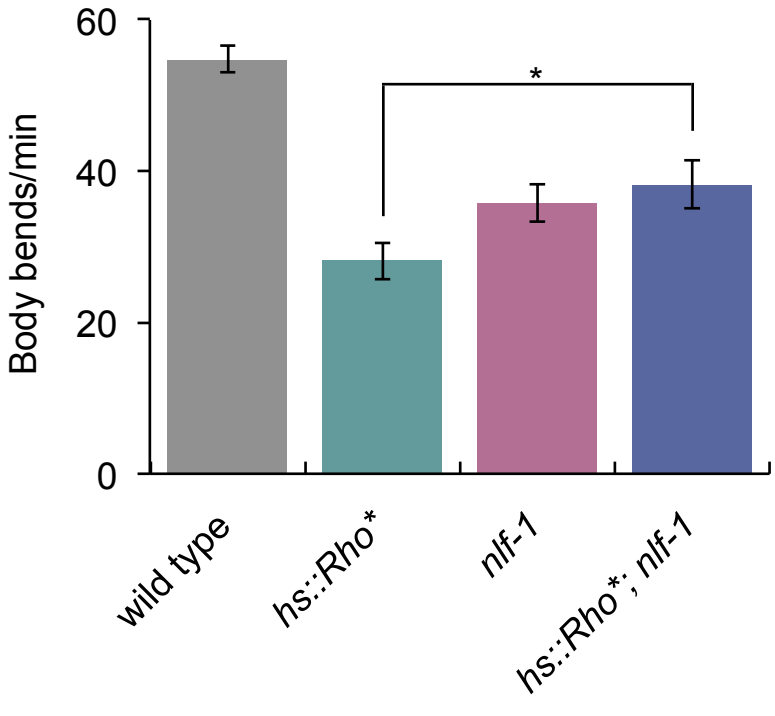

Table S1. List of strains

CB4856 Hawaiian wild isolate
EG303 *goa-1(n499 ox303) I*
EG304 *goa-1(n499 ox304) I*
EG327 *nlf-1(ox327) X*
EG330 *unc-80(ox330) V*
EG352 *nca-1(ox352) IV*
EG3447 *egl-30(tg26) I goa-1(n499) I / egl-30(tg26) I goa-1(+) I*
EG3498 *egl-30(tg26) I goa-1(n499) I / egl-30(tg26) I unc-13(e51) I gld-1(q126) I*
EG3647 *egl-30(tg26) I ; nlf-1(ox327) X*
EG3649 *egl-30(tg26) I ; unc-80(ox329) V*
EG3650 *egl-30(tg26) I ; unc-80(ox330) V*
EG3761 *unc-79(e1068) III*
EG3771 *egl-30(tg26) I ; unc-80(e1272) V*
EG3798 *egl-30(tg26) I ; egl-8(ox333) V*
EG3804 *nca-2(gk5) III ; nca-1(gk9) IV*
EG4036 *egl-30(tg26) I ; nca-2(gk5) III ; nca-1(gk9) IV*
EG4067 *goa-1(n499 ox304) I; nca-1(ox352) IV*
EG4494 *nca-1(ox352) IV ; nlf-1(ox327) X*
EG4530 *nzIs29[unc-17p::rho-1(G14V), unc-122p::gfp] II ; unc-79(e1068) III*
EG4531 *nzIs29[unc-17p::rho-1(G14V), unc-122p::gfp] II ; unc-80(ox330) V*
EG4532 *egl-30(tg26) I*
EG4681 *nzIs29[unc-17p::rho-1(G14V), unc-122p::gfp] II ; nlf-1(ox327) X*
EG4684 *nzIs1[hs::rho-1(G14V), ttx-3p::gfp] I ; unc-79(e1068) III*
EG4685 *nzIs1[hs::rho-1(G14V), ttx-3p::gfp] I ; unc-80(ox330) V*
EG4686 *nzIs1[hs::rho-1(G14V), ttx-3p::gfp] I ; nlf-1(ox327) X*
EG4690 *nzIs29[unc-17p::rho-1(G14V), unc-122p::gfp] II ; nca-2(gk5) III ; nca-1(gk9) IV*
EG4694 *unc-80(ox330) V ; nlf-1(ox327) X*
EG4697 *unc-79(e1068) III ; nlf-1(ox327) X*
EG4700 *nzIs29[unc-17p::rho-1(G14V), unc-122p::gfp] II ; nca-1(gk9) IV*
EG4718 *nlf-1(ox327) X ; oxEx1041[cosmid F55A4, unc-17p::mCherry::H2B, lin-15(+)]*
EG4733 *nca-1(gk9) IV ; vaIs46[NCA-1::GFP, lin-15+] X*
EG4761 *nzIs29[unc-17p::rho-1(G14V), unc-122p::gfp] II ; nca-2(gk5) III*
EG4782 *nzIs29[unc-17p::rho-1(G14V), unc-122p::gfp] II*
EG4783 *nca-2(gk5) III ; vaIs41[NCA-2::GFP, lin-15+]*
EG4785 *egl-30(tg26) I ; nca-1(gk9) IV*
EG4786 *egl-30(tg26) I ; nca-2(gk5) III*
EG4834 *nca-1(gk9) IV; nlf-1(ox327) X*
EG4835 *nca-2(gk5) IV; nlf-1(ox327) X*
EG4836 *nlf-1(ox327) X ; vaIs46[NCA-1::GFP, lin-15+]*
EG4837 *nlf-1(ox327) X ; vaIs41[NCA-2::GFP, lin-15+]*
EG4943 *nlf-1(ox327) X ; oxEx1146[rab-3p::nlf-1(+) cDNA::GFP, myo-2p::mCherry]*
EG5217 *oxIs412[rab-3p-FRT-mCherry-FRT-GFP-C3T, lin-15(+), hsp-FLP] II*
EG5218 *oxIs414[unc-17p-FRT-mCherry-FRT-GFP-C3T, lin-15(+), hsp-FLP] II*
EG5252 *egl-30(tg26) I ; oxIs412[rab-3p-FRT-mCherry-FRT-GFP-C3T, lin-15(+), hsp-FLP] II*
EG5263 *egl-30(tg26) I ; oxIs414[unc-17p-FRT-mCherry-FRT-GFP-C3T, lin-15(+), hsp-FLP] II*
EG5279 *oxIs434[unc-17Hp-FRT-mCherry-FRT-GFP-C3T, lin-15(+), hsp-FLP] X*
EG5287 *egl-30(tg26) I ; oxIs434[unc-17Hp-FRT-mCherry-FRT-GFP-C3T, lin-15(+), hsp-FLP] X*
EG5320 *oxIs435[unc-17βp-FRT-mCherry-FRT-GFP-C3T, lin-15(+), hsp-FLP] II*
EG5504 *nlf-1(tm3631) X*
EG5609 *egl-30(tg26) I ; rund-1(tm3622) X*

EG5611 *egl-30(tg26) I ; nlf-1(tm3631) X*
EG7249 *eri-1(mg366) IV ; lin-15(n744) X*
MT1102 *goa-1(n499) I / +*
N2 Bristol isolate, standard lab wild type
QT47 *nzIs1[hs::rho-1(G14V), ttx-3p::gfp] I*
VC9 *nca-2(gk5) III*
VC12 *nca-1(gk9) IV*
XZ1080 *egl-30(tg26) I ; unc-80(yak8) V*
XZ1113 *egl-30(tg26) I ; unc-80(yak35) V*
XZ1114 *egl-30(tg26) I ; unc-80(yak36) V*
XZ1115 *egl-30(tg26) I ; unc-79(yak37) III*
XZ1151 *egl-30(tg26) I*
XZ1152 *egl-30(tg26) I ; nuIs183[unc-129p::NLP-21-Venus, myo-2p::NLS-GFP] III*
XZ1186 *egl-30(tg26) I ; nuIs183[unc-129p::NLP-21-Venus, myo-2p::NLS-GFP] III; unc-80(yak56) V*
XZ1191 *egl-30(tg26) I ; unc-79(yak61) III nuIs183[unc-129p::NLP-21-Venus, myo-2p::NLS-GFP] III*
XZ1229 *egl-30(tg26) I ; unc-79(yak73) III nuIs183[unc-129p::NLP-21-Venus, myo-2p::NLS-GFP] III*
XZ2008 *lin-15(n765ts) X ; oxEx1144[nlf-1p::GFP, lin-15(+)]*
XZ2009 *nlf-1(ox327) X ; oxEx1147[nlf-1p::nlf-1(+)::GFP, myo-2p::mCherry]*
XZ2010 *nlf-1(ox327) X ; oxEx1149[unc-17p::nlf-1(+) cDNA::GFP, myo-2p::mCherry]*
XZ2011 *nlf-1(ox327) X ; oxEx1155[unc-17Hp::nlf-1(+) cDNA::GFP, myo-2p::mCherry]*
XZ2012 *nlf-1(ox327) X ; oxEx1151[acr-2p::nlf-1(+) cDNA::GFP, myo-2p::mCherry]*
XZ2013 *nlf-1(ox327) X ; oxEx1323[unc-17βp::nlf-1(+) cDNA::GFP, myo-2p::mCherry]*
XZ2014 *nlf-1(ox327) X ; oxEx1152[glr-1p::nlf-1(+) cDNA::GFP, myo-2p::mCherry]*

Table S2. List of plasmids

Miscellaneous plasmids

pCFJ90	*myo-2::mCherry*
pGH47	*unc-17p::mCherry::H2B*
pL15EK	*lin-15(+)*
pWD79-2RV	*hsp-16.48p::FLP*
QT#99	*Phs::GFP-C3T*
F55A4	cosmid carrying the *nlf-1* gene F55A4.2, used to make *oxEx1041* (10 ng/μl)
yk1279a1	*nlf-1* full length cDNA
Litmus 28i	
Litmus 38i	

Gateway entry clones

p_C06E1.4-93	*glr-1p* [4-1] (727 bp of the *glr-1* promoter upstream of and including the ATG)
pADA180	*unc-17Hp* [4-1] (derived from the *unc-17* promoter of pGH1, carrying a 127 bp deletion that removes the nerve cord β enhancer, expressed in head cholinergic neurons)
pCFJ31	*acr-2p* [4-1] (3362 bp of the *acr-2* promoter upstream of the ATG)
pCR110	*GFP* [1-2]
pCR185	*GFP::unc-54* 3'UTR [2-3]
pEntry[2-3]-UTR[unc-54]	*unc-54 3'UTR* [2-3]
pEntry[4-1]-P[rab-3]	*rab-3p* [4-1] (1224 bp of the *rab-3* promoter upstream of and including the ATG)
pGH1	*unc-17p* [4-1] (3229 bp of the *unc-17* promoter upstream of and including the ATG)
pMA1	*nlf-1p* [4-1] (5665 bp of the *nlf-1* promoter upstream of and including the ATG)
pMA2	*nlf-1(+)* gene with introns [1-2]
pMA3	*nlf-1* cDNA [1-2] (derived from yk1279a1)
pMA19	*C3T::unc-54 3'UTR* [2-3]
pMA23	*unc-17βp* [4-1] (a fusion of the *unc-17* nerve cord β enhancer to the minimal *unc-17* promoter consisting of the 382 bp upstream of and including the ATG, expressed in ventral nerve cord cholinergic neurons)
pWD178	*FRT::mCherry::let-858 3'UTR::FRT::GFP* [1-2]

Gateway expression constructs

pMA4	*nlf-1p::GFP*, used to make *oxEx1144* (10 ng/μl)
pMA5	*rab-3p::nlf-1 cDNA::GFP*, used to make *oxEx1146* (10 ng/μl)
pMA6	*nlf-1p::nlf-1(+)::GFP*, used to make *oxEx1147* (10 ng/μl)
pMA8	*unc-17p::nlf-1 cDNA::GFP*, used to make *oxEx1149* (10 ng/μl)
pMA9	*acr-2p::nlf-1 cDNA::GFP*, used to make *oxEx1151* (10 ng/μl)
pMA10	*glr-1p::nlf-1 cDNA::GFP*, used to make *oxEx1152* (10 ng/μl)
pMA11	*unc-17Hp::nlf-1 cDNA::GFP*, used to make *oxEx1155* (10 ng/μl)
pMA27	*rab-3p::FRT::mCherry::let-858 3'UTR::FRT::GFP::C3T::unc-54 3'UTR*, used to make *oxIs412* (10 ng/μl)
pMA28	*unc-17p::FRT::mCherry::let-858 3'UTR::FRT::GFP::C3T::unc-54 3'UTR*, used to make *oxIs414* (10 ng/μl)
pMA39	*unc-17Hp::FRT::mCherry::let-858 3'UTR::FRT::GFP::C3T::unc-54 3'UTR*, used to make *oxIs434* (10 ng/μl)
pMA40	*unc-17βp::FRT::mCherry::let-858 3'UTR::FRT::GFP::C3T::unc-54 3'UTR*, used to mak *oxIs435* (10 ng/μl)
pMA52	*unc-17β::nlf-1 cDNA::GFP*, used to make *oxEx1323* (10 ng/μl)